2004-07-13

On the Variability of the Fine Structure Constant

Jason Lott Evans
Brigham Young University - Provo

ON THE VARIABILITY OF THE FINE STRUCTURE CONSTANT

by

Jason L. Evans

A thesis submitted to the faculty of

Brigham Young University

in partial fulfillment of the requirements for the degree of

Master of Science

Department of Physics and Astronomy

Brigham Young University

August 2004

BRIGHAM YOUNG UNIVERSITY

GRADUATE COMMITTEE APPROVAL

of a thesis submitted by

Jason L. Evans

This thesis has been read by each member of the following graduate committee and by majority vote has been found to be satisfactory.

Date	Jean-Francois S. Van Huele, Chair
Date	Eric W. Hirschmann
Date	Manuel Berrondo
Date	Dallin S. Durfee

BRIGHAM YOUNG UNIVERSITY

As chair of the candidate's graduate committee, I have read the thesis of Jason L. Evans in its final form and have found that (1) its format, citations, and bibliographical style are consistent and acceptable and fulfill university and department style requirements; (2) its illustrative materials including figures, tables, and charts are in place; and (3) the final manuscript is satisfactory to the graduate committee and is ready for submission to the university library.

Date

Jean-Francois S. Van Huele,
Chair, Graduate Committee

Accepted for the Department

Scott D. Sommerfeldt,
Chair, Department of Physics and Astronomy

Accepted for the College

G. Rex Bryce,
Associate Dean, College of Mathematical
and Physical Sciences

ABSTRACT

ON THE VARIABILITY OF THE FINE STRUCTURE CONSTANT

Jason L. Evans

Department of Physics and Astronomy

Master of Science

This thesis addresses the issue of the time variability of the fine structure constant, alpha. Recent claims of a varying alpha are set against the established standards of quantum electrodynamical theory and experiments. A study of the feasibility of extracting data on the time dependence of alpha using particles in Penning traps is compared to the results obtained by existing methods, including those using astrophysical data and those obtained in atomic clock experiments. Suggestions are made on the nature of trapped particles and the trapping fields.

ACKNOWLEDGMENTS

I would like to express appreciation to Dr. Van Huele for his many hours of help in directing my research efforts and for his patient assistance with my writing. I would also like to thank Dr. Steven Turley for helping me enter the graduate program at BYU. Dr. Hirschmann's assistance with Lorentz invariance was invaluable as was Dr. Berrondo's help in calculating the the electron anomaly. Without the help of Dr. Durfee I never would have understood the intricacies of atomic clocks. Finally, I would like to publicly thank my parents for encouraging me through the years in all that I do.

Contents

List of Tables

List of Figures

Chapter 1

Introduction

Physics is full of constants. They show up in nearly every equation. They allow physicists to write two related quantities as an equality. Without this ability to write equations as equalities physics would lack the power of quantitative prediction. The constants are generally inserted into the equations by physicists. As the number of theories that rely on a particular constant increases, this constant becomes known as a fundamental constant. Even though a particular constant may show up in several theories, it is still an assumption that it really is a constant. It could be that it is approximately constant, or only constant under a given set of conditions.

However, if the previous assumption is not true, this has theoretical implications. It means that the theories are either inaccurate or incomplete, neither of which is acceptable. If, for instance, the speed of light c is time dependent, what is the effect on the Lorentz transformation? Would Lorentz invariance still be a good criterion for selecting theories?

Starting with Dirac in the nineteen thirties and continuing to current models of string theory, theorists have proposed theories with time-dependent constants. However, no experimental data have confirmed these predictions.

The experimental implications or time-dependent constants could lead to either misinterpretation of data or even contradictions. Varying constants complicate science, especially the field of metrology. The important task of continuously increasing the precision of physical constants would become meaningless because our standards would have different values at different times. As the experimentalists

reach an accuracy that is sensitive to this variation, two experiments performed only a year apart could find contradictory results for the value of the constants.

It is hard to believe that a parameter defined to be constant could actually change with time, but in 1999[9] a group of astrophysicists under John K. Webb at the University of New South Wales, Sydney, Australia, gave a convincing argument that this happens. Their claim was that the fine structure constant, α, had a larger value 10^9 years ago.

A cosmological change in alpha does not require a current variation of alpha, but the question still arises: can an earthbound laboratory experiment with high precision measure a variation of alpha? There have been several attempts by atomic clock physicists to verify this claim. However, laboratory experiments have been unable to reach the same level of precision in alpha variability measurements. The reason for this is that the added accuracy of atomic clocks cannot compensate for the large comparison times in astrophysics. The astrophysical comparison times are ten orders of magnitude larger than realistic laboratory comparison times.

There are other paths to explore the variability of alpha, such as using nuclear and geological data. I have chosen not to address these issues in this work, referring the reader to a complete review by Uzan[1].

Instead I have chosen to pursue two unexplored paths to gain new understanding on variability of the fine structure constant. First I investigated existing data to determine if it could be used and reinterpreted to detect the variability of the fine structure constant. If successful, this would clearly be the simplest and most economical method of determining the variability of alpha. Quantum electrodynamics(QED) is known for its precise measurements. Can the precision of QED be used to determine the variation of alpha? There are fifty years of electron anomaly data that could be used to calculate alpha. Fifty years of data might allow for an extended comparison time and might constrain the variability of alpha.

Second, I laid the foundation of a novel technique to obtain data on the variability of the fine structure constant by studying frequency measurements in the Penning trap and borrowing inspiration from the resonance technique used in atomic

clocks physics. The main features of this technique are spelled out in this work and arguments are presented for using specific systems in the trap. The influence of perturbing effects is also investigated, but further studies will be needed to check on the ultimate feasibility of the experiment. Readers familiar with the physics of atomic clocks and Penning traps can go straight to sections 7.4-7.6 to find the meat of the new proposal.

In this work I investigate different aspects of the variability of alpha and in particular I explore whether some ingenious laboratory experiment measuring the anomalous magnetic moment can be found to help resolve the issue.

I start out by reviewing the status of constants in physics and concentrate on, arguably, the most important one of all, alpha, the fine structure constant. Theoretical implications on the Lorentz covariance of a theory with varying alpha are explored in Chapter 3. In Chapter 4, I review the precision data that are currently available in QED to determine if new experiments are really needed to decide on the variability of alpha or whether existing data are sufficient. Then I analyze the astrophysical method in Chapter 5. In Chapter 6, I study two particular methods of extracting alpha variability data using atomic clocks. I discuss in some detail the geonium experiments that measure the electron anomaly in Chapter 7. Finally in Chapter 8, I compare the advantages and disadvantages of three methods for measuring the variability of the fine structure constants and offer final conclusions. In the appendices I review the derivation of the value of g, the Landé factor predicted by Dirac, and $g-2$, the first order electron anomaly, as predicted by Schwinger. Tables and figures appear where they belong in the text and are listed separately in the introductory pages of the thesis.

Chapter 2

Constants and Alpha

As already stated, physics is full of constants. In order to relate two separate quantities that arise in experiment, the necessity of using constants appears. The constants make these relations into an equality. They transform a qualitative statement into a quantitative one. The more accurately the constants are known, the more exact the relation is. In this chapter we define what it takes to be a fundamental constant and introduce the fine structure constant, α.

2.1 Constants of Physics

Constants that appear very frequently are given the name of fundamental constants. Examples of these fundamental constants are c, h, and e. Here c is the speed of light, the constant that defines relativity; h is known as Planck's constant, it can be said to define quantum theory, and e is the smallest increment of free electric charge that can be measured. These constants, and a handful of others, play a crucial role in defining the most fundamental theories of physics. Hence, they are known as fundamental constants.

Although it would seem that a particular constant would have a defined magnitude, this is not the case. Most constants take on different values depending on the units they are displayed in. This means that the actual value of the constant will vary from unit system to unit system. An example of this is g, the gravitational acceleration. In SI units g is about $9.80 m/s^2$, but in Imperial units it is $32 ft/s^2$. This leaves a lurking ambiguity in the magnitude of constants with units. An example where this leads to problems is in the conversion of joules(J) to electron volts(eV). The

conversion factor for this change of units is the charge of the electron. The problem arises because of the limited accuracy on the charge of an electron. This means that a measurement made in one unit system may not be converted to a measurement in another unit system with equal accuracy.

Some constants in physics are dimensionless. Because dimensionless constants have no units, the magnitude will be unaffected by a change of units, thus removing the previously mentioned ambiguity. This has led to the belief that dimensionless constants play a more fundamental role in physics. An example of a unitless constant is the Reynolds number. The Reynolds number

$$R_e = \frac{\rho v l}{\eta}, \tag{2.1}$$

is used to determine the conditions under which fluid flow will become turbulent. It is dependent on ρ, the density, v, the velocity, η, the viscosity, and l, the linear dimension of the system. Because this constant is independent of the units used, they do not play a role in its value. The physics of turbulent flow can now be defined in terms of its fundamental aspects without the consequences of changing units. This allows experimental work to be done on smaller models with the assurance that the results will translate to larger objects if the variables are modified so as to leave this particular combination unchanged.

Another unitless constant, but of more foundational importance to physics, is the fine structure constant, α. It is more fundamental than the Reynolds number because it shows up in theories dealing with relativity, quantum theory, and electromagnetism. Another more fundamental aspect of α is that it is unique: it retains the same value for all theories and systems. The fine structure constant has the form

$$\alpha = \frac{e^2}{\hbar c}. \tag{2.2}$$

As an aside we note that some texts define

$$\alpha = \frac{e^2}{4\pi\epsilon_0 \hbar c}, \tag{2.3}$$

because of their choice of electromagnetic units. This does not affect our conclusion since α is still dimensionless under both definitions and still retains the same value for all units.

2.2 Time Dependent Constants

Because we believe that physics today is the same as yesterday, it seems absurd to think that something such as a constant would have time dependence. However, there are people that have considered just that.

2.2.1 Theoretical Search for Time Dependent Constants

When Dirac examined a complete set of unitless constants, composed of ratios of what he believed to be the most fundamental constants, he found that they split into two groups of different magnitudes. The values in these groups were separated by many orders of magnitude. This led Dirac to believe that these groups were very fundamental. One of the constants Dirac considered to be of fundamental importance was Hubble's constant. Hubble's constant is time dependent. To preserve the fundamental importance of the groups, Dirac proposed that the other member of the group must be time dependent as well. This led Dirac to propose that the gravitational constant G is time dependent[3].

This suggestion has led others to consider the possibility of time dependent constants. Even the quickly growing field of string theory suggest that some constants may be time dependent[6].

2.2.2 Experimental Search for Time Dependent Constants

The experimental search for time dependent constants is moving forward on at least two fronts. The first method, used by astrophysicists, is to use large time scales that will magnify the change. This method has led at least one group to propose a time dependent fine structure constant [9].

The other method uses high precision measurements that are run on much shorter time scales. This method has the advantage of greater control over the experiment, but lacks the large times scales allowed in the astrophysical observation.

These two methods raise the question as to whether they are really measuring the same thing. If the fine structure constant underwent change in the early universe but this change has levelled off, these two methods would give different answers. At this stage, however, each method must still push forward to a greater degree of precision before we can resolve this question.

2.3 The Fine Structure Constant

The first place where the fine structure constant showed up was in the splitting of the energy levels in atoms [13]. This fine structure removes the degeneracy of given energy levels by splitting them into levels with different total angular momentum.

As is seen in figure 2.1 the $n = 2$ level of the hydrogen atom splits so that the p states with $j = 3/2$ are no longer degenerate with the other p and s states with $j = 1/2$. This can be seen in the formula for the energy of the fine structure

$$E_{jn}^{fs} = \frac{mc^2\alpha^4}{8n^4}\left[3 - \frac{3}{j+1/2}\right], \tag{2.4}$$

where j is the quantum number for the total angular momentum. This is a contribution that supplements the energy predicted by Schrödinger. The energy levels predicted by the Schrödinger's equation are [12]

$$E_n = -\alpha^2\frac{mc^2}{2n^2}. \tag{2.5}$$

The fine structure constant has a value of approximately 1/137. This means that the energy splitting of the fine structure is of order α^2 or approximately 10^{-4} the size of the energy level separation predicted by Schrödinger. Experimentally this is the first place that the fine structure constant appeared. However, it is also present in the hyperfine splitting, the Lamb shift [14] and almost everything that has its origin in Quantum Electrodynamics (QED).

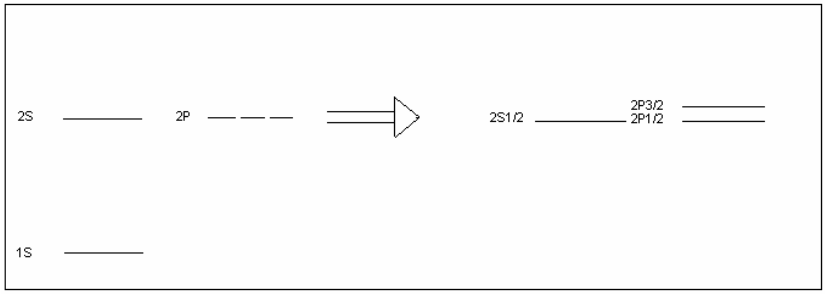

Figure 2.1: Energy splitting of the hydrogen n=2 states according to Schrödinger (left) and Dirac (right)

2.4 Time Dependent Fine Structure Constant

Although the origin and even the name of the fine structure constant suggest that it is independent of time, this cannot be taken for granted. One of the first suggestions that alpha was time dependent was proposed by string theorists. Many forms of string theory allow for and even require a time dependent fine structure constant. This has led to many experimental searches for this time dependence of the fine structure constant. Before 1999[9] there was no experimental evidence to vindicate the string theorists' claims. In 1999 John K. Webb found evidence of a time dependent fine structure in the spectra of quasars[9].

Chapter 3

Investigation of Lorentz Covariance

If the astrophysical claim that the fine structure constant is changing is correct, what is the origin of the variation of the fine structure constant? As was stated earlier the fine structure constant is composed of three other fundamental constants e, the charge of an electron, h, Planck's constant, and c, the speed of light. The search for the origin of this variation of the fine structure constants can be rephrased as a search for which one or more of these three constants is changing [34].

It seems very unlikely that the charge of an electron is changing. The reason for this view stems from the fact that charge is ultimately just a counting unit due to the quantization of charge. It counts the number of electrons (or protons). Coulomb's force law could really be rewritten in the form of a number of electrons (or quarks) times some other factors. This form of Coulomb's law would work just as well as the currently accepted form. If Coulomb had known that the charge of an electron was quantized the charge of an electron would most likely be one. Now it seems unlikely that one electron in the future will be a fraction of an electron in a million years. This would suggest that charge is more than a counting unit, a notion that we reject[34].

Another unlikely candidate for alpha's time dependence is Planck's constant. An argument against h-variation goes like this: quantum systems are entangled, with h being a measure of the degree of entanglement. This entanglement links all systems and a variation of h in space-time would require noticeable and completely new time dependent results here on earth[34].

This has led some (Peres[34]) to suggest that the cause of alpha variation is a varying speed of light, c. One can argue that the speed of light is really just a

scaling factor between space and time. There would be little difference between a world where c was constant and a world where c was time dependent. The difference would be in the degree of relativistic effects, not in a manifestation of new effects. In the next section we explore the possibility of a time-dependent speed of light.

3.1 Lorentz Transformation

In the early twentieth century it was apparent that the laws of electricity and magnetism were not invariant under a Galilean transformation. Because of this, many physicists believed that electromagnetic fields were propagating through a fluid known as the ether. The ether would explain the lack of invariance in Maxwell's equations under a Galilean transformation since the ether frame would be the only frame in which Maxwell's equations would be valid. In spite of this strong belief, Michelson and Morley were unable to measure the speed of the earth through the ether. Lorentz found a transformation of space-time, the Lorentz transformation, that keeps Maxwell's equations invariant. However, Lorentz still believed in the ether. It wasn't until Einstein proposed his theory of special relativity that Lorentz transformations were given proper footing as a statement about a transformation between values observed by different observers, rather than a physical transformation of space and time. Since that time, Lorentz transformations have become a very fundamental aspect of physics and Lorentz invariance is used as a criterion for selecting theories.

3.2 Time Dependent Lorentz Transformations

In examining the consequences of a time varying speed of light on current electromagnetic theory, I first look at the effect on Lorentz transforms themselves, because of their foundational importance. The origin of the Lorentz transformation is rooted in a belief that the laws of electricity and magnetism are the same for all observers. Because of this, I investigate the Lorentz invariance of Maxwell's equations if a time dependent speed of light is assumed. Is it conceivable that there exist a time-dependent speed of light that is still consistent with Maxwell's equations and the form

of the Lorentz transformation? To test for invariance, Maxwell's equations for a field $F^{\mu\nu}$ in the presence of a current J^{ν}

$$\partial_{\mu}F^{\mu\nu} = \mu_0 J^{\nu}, \tag{3.1}$$

where μ_0 is the permeability of free space, are transformed into a new reference frame using the the Lorentz transformation in matrix form

$$\Lambda^{\mu}_{\nu} = \begin{pmatrix} \gamma & -\gamma\beta & 0 & 0 \\ -\gamma\beta & \gamma & 0 & 0 \\ 0 & 0 & 1 & 0 \\ 0 & 0 & 0 & 1 \end{pmatrix}, \tag{3.2}$$

where

$$\beta = \frac{v}{c}, \tag{3.3}$$

and

$$\gamma = (1 - \beta^2)^{1/2}. \tag{3.4}$$

Identifying the matrix elements in Eq. (3.1) as tensorial components, we get

$$\Lambda^{\sigma}_{\nu}\partial_{\mu}F^{\mu\nu} = \Lambda^{\sigma}_{\nu}\mu_0 J^{\nu}. \tag{3.5}$$

This is followed by a transformation of the derivatives, tensors and vectors of the equation, leading to

$$\Lambda^{\sigma}_{\nu}\Lambda^{\alpha}_{\mu}\partial_{\alpha}\left[\Lambda^{\mu}_{\delta}\Lambda^{\nu}_{\eta}F^{\delta\eta}\right] = \Lambda^{\sigma}_{\nu}\mu_0\Lambda^{\nu}_{\beta}J^{\beta}. \tag{3.6}$$

If a time or position dependence of the speed of light is assumed, then the derivative can no longer pass up the Lorentz transformation matrices, because they have become space and time dependent. The product rule can be used which leads to the following equation

$$\Lambda^{\sigma}_{\nu}\Lambda^{\alpha}_{\mu}\Lambda^{\mu}_{\delta}\Lambda^{\nu}_{\eta}\left(\partial_{\alpha}F^{\delta\eta}\right)+\Lambda^{\sigma}_{\nu}\Lambda^{\alpha}_{\mu}F^{\delta\eta}\left(\partial_{\alpha}\Lambda^{\mu}_{\delta}\Lambda^{\nu}_{\eta}\right)=\Lambda^{\sigma}_{\nu}\mu_{0}\Lambda^{\nu}_{\beta}J^{\nu}. \tag{3.7}$$

From the property of Lorentz transformations

$$\Lambda^{\sigma}_{\mu}\Lambda^{\mu}_{\alpha}=\delta^{\alpha}_{\sigma}, \tag{3.8}$$

Eq. (3.9) becomes

$$\partial_{\alpha}F^{\alpha\sigma}+\Lambda^{\sigma}_{\nu}\Lambda^{\alpha}_{\mu}F^{\delta\eta}\left(\partial_{\alpha}\Lambda^{\mu}_{\delta}\Lambda^{\nu}_{\eta}\right)=\mu_{0}J^{\sigma}. \tag{3.9}$$

Maxwell's equations will be invariant if

$$F^{\delta\eta}\Lambda^{\sigma}_{\nu}\Lambda^{\alpha}_{\mu}\partial_{\alpha}\Lambda^{\mu}_{\delta}\Lambda^{\nu}_{\eta}=0 \tag{3.10}$$

for all values of σ, the only fixed index.

If the speed of light is considered to be time dependent only, and not space dependent, then the derivatives become ∂_0. Because Lorentz transformations are ultimately functions of β, Eq. (3.10) can be reduced to

$$F^{\delta\eta}\Lambda^{\sigma}_{\nu}\Lambda^{0}_{\mu}\frac{\partial}{\partial\beta}(\Lambda^{\mu}_{\delta}\Lambda^{\nu}_{\eta})\frac{d\beta}{dt}=0. \tag{3.11}$$

Everything to the the left of the time derivative of β can be divided out, leading to an equation of the form

$$\frac{d\beta}{dt}=0. \tag{3.12}$$

The only solution to this is a constant β. If β is constant, then it is required that c be a constant as well.

One of the consequences of relativity is that it places space and time on the same footing. This leads to the question of whether the Lorentz transformation allows for a space-time dependent speed of light. This means that Eq. (3.10) must be shown to be satisfied for all values of σ and α. This is done by summing over the repeated indices. Setting $\sigma = 0$ and summing over all other indices in Eq. (3.10), the following differential equations is found

$$F^{31}\partial_3\beta + F^{21}\partial_2\beta = 0. \tag{3.13}$$

Because F^{31} and F^{21} are completely independent of one another, the terms multiplying them must each be zero separately. This leads to the conclusion that the derivatives of β with respect to y and z are zero. This means that β is independent of y and z and therefore c is independent of y and z. Setting $\sigma = 2$, the following differential equation is found

$$F^{02}\partial_1\beta + F^{12}\partial_0\beta = 0. \tag{3.14}$$

F^{02} and F^{12} are also completely independent of each other and therefore their multiplying coefficients must be zero. This also leads to the conclusion that the derivatives of β with respect to x and t are zero, implying that β is independent of x and t and therefore c is independent of x and t.

The conclusion is that a constant speed of light is necessary for Lorentz invariance. However, this is not so alarming to many physicists today. Many current theories require a local breaking of Lorentz invariance[6].

Chapter 4

Fifty Years of g-2

In recent years astronomical observations have been presented that make a case for a time dependent α. Because of the difficulty in interpreting astronomical data, physicists are looking for an experiment that can be performed in a laboratory to help substantiate or disprove the astronomical observations. However, this task is very difficult. The astrophysicists have an advantage because they are able to use large comparison times that are on the order of 10^9 years. On the other hand, laboratory experiments have the advantages of repeatability and greater control over the experimental environment. Is it possible to incorporate the advantages of these two regimes simultaneously, creating the best possible method for measuring a variation in the fine structure constant? In an attempt to use these two advantages I have combined the $g-2$ data which comes from earth bound experiments, considered them over the past fifty years (giving a comparison time of about 10^2) and used them to check for alpha variability.

4.1 Fine Structure

The Schrödinger equation predicts that in hydrogen, electrons with the same principal quantum numbers have the same energy. However, the relativistic kinematical correction and the spin-orbital correction split degenerate states by lifting the degeneracy.

This splitting of energy levels is called the fine structure of an atom and it is proportional to the square of a unitless constant called the fine structure constant α, where

$$\alpha = \frac{e^2}{\hbar c}. \tag{4.1}$$

4.2 QED and g-2

The spin magnetic moment $\vec{\mu}_s$ of an electron is related to its spin angular momentum $\vec{S}$ through the following formula:

$$\vec{\mu}_s = -g\frac{e}{2m}\vec{S}. \tag{4.2}$$

Here, m is the mass of an electron, e is its charge, and g is its Landé factor. Using Dirac's relativistic quantum mechanics, the Landé factor is predicted to be exactly 2 for an electron. My derivation of this result is presented in Appendix A. However, the current experimental value is 2.002319304 for the Landé factor [32]. The extra contribution to the magnetic moment found in the Landé factor is called the anomalous magnetic moment. Quantum Electrodynamics (QED) is able to predict the anomalous magnetic moment very precisely. The electron anomaly a_e is defined as

$$a_e = \frac{g-2}{2}, \tag{4.3}$$

where g is the Landé factor. The electron anomaly would be zero for a pure Dirac electron.

In the theory of Quantum Electrodynamics (QED) the anomalous magnetic moment and the fine structure constant are related. The relation can be illustrated by considering corrections to the vertex of QED. The vertex diagram of QED represents a travelling particle which has either absorbed or emitted a quantum of light. The elementary vertex, which involves only one interaction, can be seen in figure 4.1. A derivation of the contribution of this diagram is given in Appendix B.

The corrections to the vertex incorporate an increasing number of interactions. The lowest order correction to the vertex can be seen in figure 4.2.

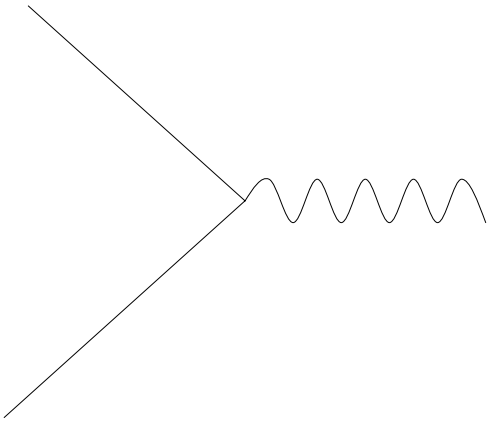

Figure 4.1: The elementary vertex of QED

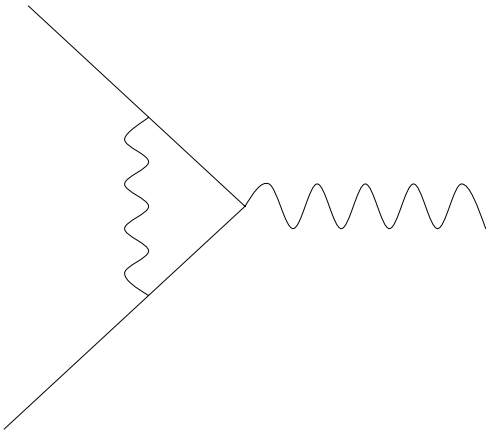

Figure 4.2: The first correction to the elementary vertex of QED

Higher order corrections to the vertex, which have a larger number of lines and interactions, contribute less to the anomalous magnetic moment. Each new photon line in a Feynman diagram involves new elementary vertices and each pair of vertices in a Feynman diagram contributes a factor of α. The calculation of all Feynman diagrams with every possible interaction leads to a perturbative series in alpha . However as the diagrams become more complicated they involve an increasing number of elementary vertices. The paths now involve the creation and annihilation of particles, in the virtual sense. An example of this would be the creation and annihilation of an electron and a positron pair. However, one should consider all charged particles, since they all interact with the electromagnetic field. As the particles created become more massive, their contribution to the anomalous magnetic moment decreases. This can be understood in terms of the energy required for a particle to take a given path. The paths that involve heavier particles require more energy and are therefore less likely to happen. The lowest energy contributions to the anomalous magnetic moment in QED can be grouped into four groups as follows [28]:

$$a_e = A_1 + A_2(m_e/m_u) + A_2(m_e/m_\tau) + A_3(m_e/m_\mu, m_e/m_\tau), \tag{4.4}$$

where the parameters refer to functional dependence.

The first term, labelled A_1, is the contribution to the anomalous magnetic moment due to photon interaction with electron and positron pairs only. Because this term involves interactions with photons only, it will be the largest contribution to the anomalous magnetic moment. The term $A_2(m_e/m_\mu)$ is the contribution to the magnetic moment from interactions involving electrons, muons, and their antiparticles. Because this term involves diagrams with heavier particles being created and destroyed it will contribute less than A_1. $A_2(me/m_\tau)$ is the contribution to the anomalous magnetic moment of interactions involving electrons, tauons, and their antiparticles. $A_3(m_e/m_\mu, m_e/m_\tau)$ is the contribution to the anomalous magnetic moment of electrons, muons, tauons, and their antiparticles all in a single diagram. This

term will contribute the least of the four because of the very massive particles involved. Each of these terms in Eq. (4.4) is composed of an infinite series of the form

$$A_i = \sum_{n=1}^{\infty} A_i^{(2n)} (\frac{\alpha}{\pi})^n, \tag{4.5}$$

where the coefficients $A_i^{(2n)}$ carry the mass dependence.

The coefficients in the series of alpha are determined from calculations of the respective Feynman diagrams. The first three coefficients of the series for A_1 have all been determined analytically and many of the other terms have been calculated numerically. The coefficients determined numerically have an added uncertainty associated with them[28]. The strong and weak particle contributions have been neglected in Eq. (4.4) because they are small.

4.3 Astrophysical Evidence of Changing Alpha

In recent years, Webb et al. claimed to have detected a variation of the fine structure constant. Comparing Mg and Fe lines in quasar data with the corresponding current values, Webb et al. measured an average change of $\Delta\alpha/\alpha = (-1.1 \pm 4) \times 10^{-5}$ for a red shift of z=.5 to 3.5 where z is defined as

$$z = \sqrt{\frac{1+\beta}{1-\beta}} - 1, \tag{4.6}$$

and $\Delta\alpha$ is

$$\Delta\alpha = \alpha_0 - \alpha_z \tag{4.7}$$

where α_0 is the current α and α_z is the value of α at the corresponding redshift z.

4.4 Calculation of Alpha From g-2 Data

From Eq. (4.3)-(4.5) the fine structure constant can be solved for in terms of the anomalous magnetic moment and the coefficients of the perturbative series. Using the data that is available for the anomalous magnetic moment since the 1940's[27],

a plot of alpha versus time can be made. Because of the complexity of this formula and the fact that it is a perturbative series, I only consider the contributions to the anomalous magnetic moment from the A_1 terms. As explained above, the terms involving massive particles are much higher in energy and hence contribute much less to the calculation of the anomalous magnetic moment. I begin my calculations by only giving consideration to the term linear in alpha of the A_1 contribution to the anomalous magnetic moement. This leads to an equation for inverse alpha of the form:

$$\frac{1}{\alpha} = \frac{1}{2a_e\pi} \tag{4.8}$$

where a_e is the anomalous magnetic moment. Using this relationship and the $g-2$ data from the past fifty years, I plot inverse alpha versus time. I then determine the error of the inverse of alpha due to the error on the measurement of the anomalous magnetic moment as reported in the experimental publications. I then plot inverse alpha with inverse alpha plus the error and with inverse alpha minus the error on the same graph as inverse alpha. The error takes the form

$$\Delta\frac{1}{\alpha} = -\frac{\Delta a_e}{2a_e\pi}. \tag{4.9}$$

This allows for a comparison between Webb et al.'s predicted slope and the $g-2$ data. I repeat the analysis keeping both the linear and quadratic terms in α in Eq.(4.5). This approximation gives a formula of

$$\frac{1}{\alpha} = \frac{2A_1^{(4)}}{\pi\left(-A_0^2 + \sqrt{(A_0^{(2)})^2 + 4A_1^{(4)}a_e}\right)} \tag{4.10}$$

where a_e is the anomalous magnetic moment and the $A_i^{(2n)}$ terms are defined in Eq.(4.5). The error for this approximation is determined by taking a derivative of the inverse alpha relation

$$\Delta\frac{1}{\alpha} = \frac{4(A_1^{(4)})^2\Delta a_e}{\pi\left(-A_0^2 + \sqrt{(A_0^{(2)})^2 + 4A_1^{(4)}a_e}\right)^2\sqrt{(A_0^{(2)})^2 + 4A_1^{(4)}a_e}}. \tag{4.11}$$

A plot of inverse alpha and inverse alpha plus or minus the error is given in figure 4.3. The same procedure was used in calculating the value of inverse alpha in a third order approximation with similar result. Because of increasing complexity and the lack of significant increase in accuracy due to fourth order terms in alpha and higher, these approximations are not calculated. The plot of the third order approximation is shown in figure 4.3.

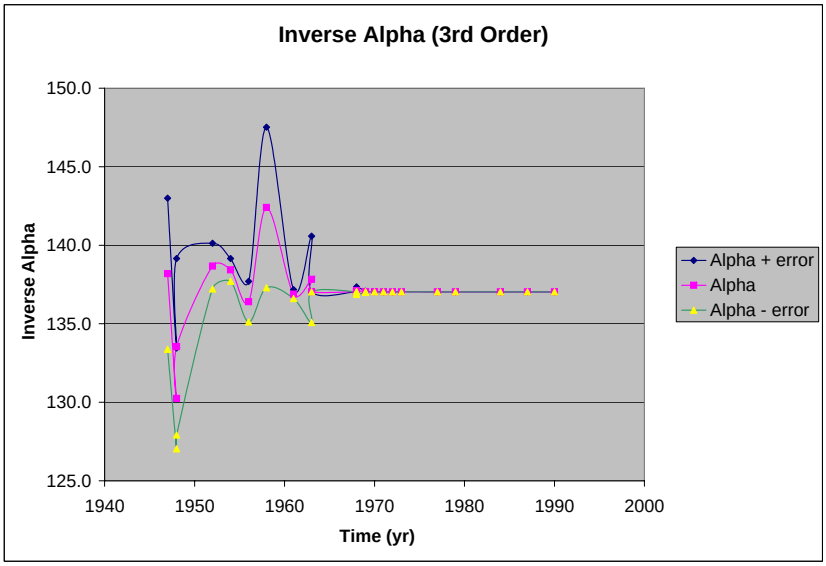

Figure 4.3: Alpha data from QED since 1950

The data before 1975 has extremely large error bars, making it unhelpful in constraining the variability of alpha. Some of the results appear to be wrong because they are not consistent with other measurements of the electron anomaly. Because of

this lack of accuracy, I discard the data before 1975 and plotted the rest of the data, as seen in figure 4.3.

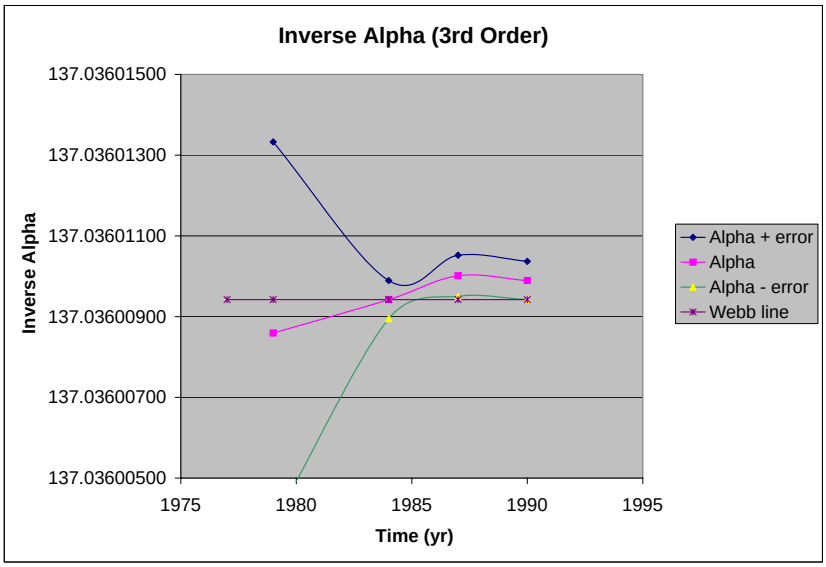

Figure 4.4: Alpha data from QED since 1978

However, the data since 1975 was not accurate enough to confirm the variation that was presented by Webb et al.. The reason for this is that the data is only as good as the worst data point for the time period considered. This means that, for data after 1975, the oldest point really determines the level of accuracy. And as is seen in figure 4.4 even the later more accurate data is unable to compete with the accuracy of astrophysical measurement.

Chapter 5

Astrophysical Claims on Alpha Variability

5.1 Motivation

In search of an experimental method to verify string theory claims that the fine structure constant might be time dependent, a group in Australia under John K. Webb analyzed astrophysical data from quasars[9]. In this chapter we will present the method that led astrophysicists to claim that α is changing and we will show their data. To end the chapter we will also present some astrophysical data that contradict these original claims and conclude on the status of α variability from astrophysics.

5.1.1 Quasars

The name quasar comes from the contraction of QuAsi-Stellar Radio Sources. Quasars were originally discovered as an intense point-like source of radio waves [35]. Because of the large intensities measured, they were originally believed to be stars in our galaxy. However, it has been discovered that quasars are actually very distant objects and therefore extremely intense. They are now believed to be radiation signals from the center of a galaxy. This radiation indicates the formation of a black hole. These black holes are surrounded by large clouds of dust. These dust particles are pulled in by the forming black hole. As these particles are pulled in, they orbit due to the presence of a strong magnetic field. This orbital motion causes synchrotron radiation in the form of radio waves. This radiation is selectively absorbed by the surrounding gas clouds. This absorption leads to a spectrum that can then be analyzed by astronomers.

5.1.2 Analysis

In order to obtain a significant constraint on the variability of the fine structure constant one needs either very precise experiments or very long comparison times. Long comparison time will magnify the variation and so accommodate less accurate measurements. Quasars are only present in emissions that are over 1 billion years ($10^{16}s$) old. This allows for comparison on large time scales and makes quasars good candidates for testing the variability of the fine structure.

The methods that was previously used for detecting time variations of α consisted in detecting variations of the relativistic fine structure splitting of alkali-type doublets (AD). The separation of the lines in one multiplet is proportional to α^2. Thus small variations in the separation are proportional to α [9]. This can be understood by examining the following energy separation equation

$$E_2 - E_1 = A\alpha^2. \tag{5.1}$$

This energy separation leads to a time dependent frequency that is proportional to alpha in the following way

$$\frac{d\omega}{dt} = \frac{1}{\hbar}\frac{d(E_2 - E_1)}{dt} = \frac{2A\alpha}{\hbar}\frac{d\alpha}{dt}. \tag{5.2}$$

In order to gain accuracy Webb et al. compares wavelengths in transitions belonging to different ions, in particular transitions from MgII and FeII that are commonly seen in quasar signals. They develop a procedure for simultaneously analyzing the spectra of MgII and FeII. The transitions used by Webb et al. are "MgII 2796/2803 doublet and up to five of FeII transitions,(FeII 2344,2374,2383,2587, 2600 Å), from three different multiplets" [9]. The advantage of a comparative technique is that MgII transitions frequencies are one order of magnitude less sensitive to variations in alpha than the transition in FeII. Magnesium is less sensitive because the coefficients in the expression for the energy transitions are an order of magnitude smaller. This means that the magnesium atom acts as a reference with which to gauge the variation of the iron transitions. The comparison decreases the uncertainty

in the measurement and allows for smaller error bars in the data. The energy equation used by Webb et al. to assess the variation of the fine structure constant is

$$E_z = E_{z=0} + [Q_{i_1} + K_{i_1}(\mathbf{LS})]\, Z^2 \left[\left(\frac{\alpha_z}{\alpha_0}\right)^2 - 1\right] + K_{i_2}(\mathbf{LS})^2 Z^4 \left[\left(\frac{\alpha_z}{\alpha_0}\right)^4 - 1\right], \quad (5.3)$$

where Z is the nuclear charge, $\mathbf{L}$ and $\mathbf{S}$ are the orbital and spin angular momentum respectively and α_0 and α_z are defined in section 4.3. The coefficients Q_{i_1} are relativistic coefficients that are calculated numerically from a many body theory. K_{i_1}, and K_{i_1} are relativistic spin orbit coefficients. The different coefficients for each transition are denoted by the index i. If the coefficients for each transition are determined, the equations for the transition frequencies in magnesium become

$$\begin{aligned} MgII \;\; {}^2P \qquad & J = 1/2: \;\; \omega = 35669.289(2) + 119.6x \\ & J = 3/2: \;\; \omega = 35760.835(2) + 211.2x \end{aligned} \quad (5.4)$$

and the equation for the transition frequencies in iron become (Adapted from Webb et al.[9])

$$\begin{aligned} FeII \;\; {}^6D \qquad & J = 9/2: \;\; \omega = 38458.9871(20) + 1394x + 38y \\ & J = 7/2: \;\; \omega = 38660.0494(20) + 1632x \\ {}^6F \qquad & J = 11/2: \;\; \omega = 41968.0642(20) + 1622x + 3y \\ & J = 9/2: \;\; \omega = 42114.8329(20) + 1772x \\ {}^6P \qquad & J = 7/2: \;\; \omega = 42658.2404(20) + 1398x - 13y, \end{aligned} \quad (5.5)$$

where $x = \left[\left(\frac{\alpha_z}{\alpha_0}\right)^2 - 1\right]$ and $y = \left[\left(\frac{\alpha_z}{\alpha_0}\right)^4 - 1\right]$. Using the data from quasars the α_z is determined which will best fit each of the previous seven equations simultaneously.

5.2 Data

The original paper presented by Webb et al. that proposed a time varying fine structure constant involved a survey of 25 different quasars. These quasars had

a redshift range of $.05 < z < 1.6$. If the entire sample is averaged a variation of $\Delta\alpha/\alpha = -1.1 \pm 0.4 \times 10^{-5}$ is found. However the variation is dominated by the measurement with $z > 1$, where $\Delta\alpha/\alpha = -1.9 \pm 0.5 \times 10^{-5}$. The variation for the measurement with $z < 1$ is $\Delta\alpha/\alpha = -0.2 \pm .04 \times 10^{-5}$, which is consistent with a constant α.

To further their case for a varying fine structure constant, Webb et al. increased the redshift range to $0.5 > z > 3.5$. In order to increase their sample size, it was necessary to alter their original experiment for the redshift range of $1.8 < z < 3.5$. Instead of using a comparative technique of FeII and MgII for this range they now used NiII, CrII and ZnII. They also considered some older techniques for measuring the variability of α as can be seen in Table 5.1.

Sample	Method	N_{abs}	Redshift	$\Delta\alpha/\alpha(10^{-5}$
FeII/MgII	MM	28	$0.5 < z < 1.8$	-0.70 ± 0.23
NiII/CrII/ZnII	MM	21	$1.8 < z < 3.5$	-0.76 ± 0.28
FeIV	AD	21	$2.0 < z < 3.0$	-0.5 ± 1.3
21cm/mm	radio	2	0.25,0.68	-0.10 ± 0.17

Table 5.1: A comparison of different methods for measuring the variation of alpha for different redshifts. Adapted from Webb et al. [8]

If the data sets are binned into groups with similar redshifts, this leads to the plot that can be seen in figure 5.1.

The graph clearly shows a variation of the fine structure constant, with increasing effect as the red shift grows larger. However, as the redshift grows larger, the error bars also become larger.

Although Webb et al. concluded that the fine structure constant is changing using the Multiplet Method (MM), recently other researchers [11] have also published

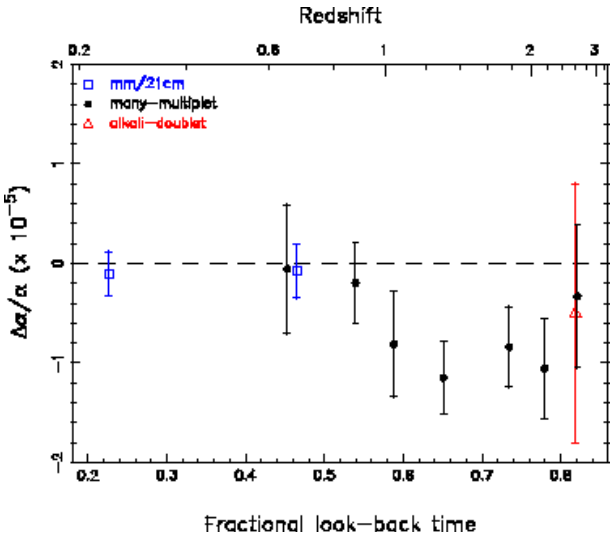

Figure 5.1: The plot after the binning of quasar data (adapted from [8])

results using this method. In order to verify the sensitivity of their results, these researchers first fabricated data that corresponded to a varying fine structure constant. They then used this data to test the accuracy of MM. They found that, when using the comparison technique of MM, it is best to compare multiplets that act as singlets. This gave criteria from which to select quasars for analysis. Using these criteria, 18 quasars were selected for analysis using MM. This led to a variation of alpha of $\Delta\alpha/\alpha = -0.06 \pm .06 \times 10^{-5}$ for a red shift of $04 < z < 3.4$.

Therefore, later work by different astrophysical groups seem to significantly decrease the solidity of the original claim. However, it should be noted that Webb et al. has mentioned that systematic effects could be present and has made an effort to remove them.

Chapter 6

Atomic Clocks and Alpha Variability

Currently the best method for determining the variability of the fine structure constant from an earth bound experiment comes from atomic clock measurements.

6.1 Two Methods

Atomic clock measurements can be broken into two separate categories. One method involves the comparison of transitions present in two different atoms[22]. The other method involves the comparison of two different transitions with nearly equal transition frequencies that are in the same atom[25]. Both of these methods have allowed atomic clock physicists to lead the way in the measurement of alpha variability in laboratory experiments. We review briefly the principles on which both methods are based and we compare their results. We will get some of our inspiration for the method we develop in Chapter 7 from the nearly degenerate level method.

6.1.1 Comparison of Hyperfine Splitting in Different Atoms

The theory of atomic clocks is based on a comparison of two separate clocks. To understand this need for a comparison let us consider a wrist watch and a clock on the wall. If the wrist watch is running slow, how do I know it is running slow? I have no way of knowing it is running slow unless I compare its time measurement to another clock, such as the clock on the wall. Because different atomic clocks have a different dependence on α, if α is changing, they will "slow" at different rates. This means a change in α will be observed as one of the clocks running slow.

One type of atomic clock that is used in this manner is based on the frequency of the hyperfine splitting of two different atoms A and B. Time is measured by first defining a length of time, say a second, as a certain number of periods of the hyperfine frequency in atom A.

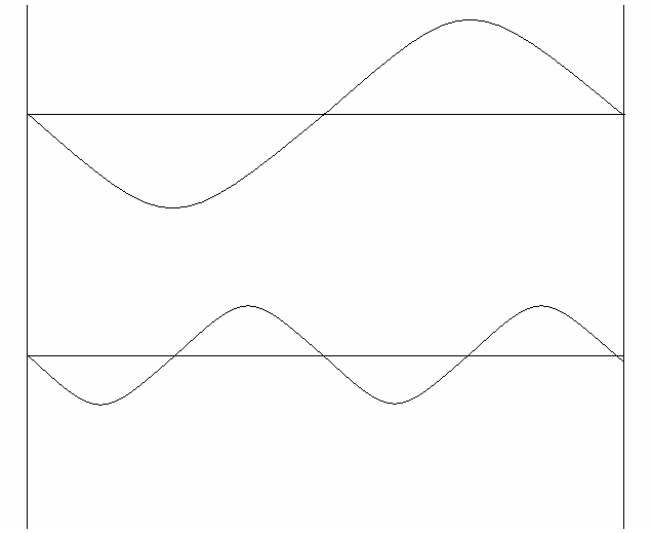

Figure 6.1: Node comparison between two clocks

Time is defined in terms of the number of nodes of the electromagnetic wave of the hyperfine transition see figure 6.1. These frequencies can be determined to approximately 1 part in 10^{15} leading to a very sensitive method for detecting frequency drift and hence a variability of alpha.

The formulas for the frequencies associated with hyperfine splitting is very complicated with coefficients depending on physical parameters that contain large error bars[22]. However, this difficulty can be overcome when a ratio of frequencies is considered. This ratio provides a way of comparing two frequencies and will allow for detection of a relative frequency drift. Any frequency drift found in this manner

would indicate a varying alpha. The general expression for frequency, A_s of a hyperfine splitting in an atom of atomic number Z is

$$A_s = \frac{8}{3}\alpha^2 g_l Z \frac{z^2}{n_*^3}\left(1 - \frac{d\Delta_n}{dn}\right) F_{rel}(\alpha Z)(1-\delta)(1-\epsilon)\frac{m_e}{m_p}R_\infty c. \tag{6.1}$$

The $g_I l$ term is the nuclear Landé factor, m_e and m_p are the electron mass and proton mass respectively, $R_\infty c$ is the Rydberg constant in frequency units, z is the the net charge of the remaining ion after removing valence electrons, n_* is the effective quantum number, and $\Delta_n = n - n_*$ is the quantum defect for the nth state. The term $1-\delta$ corrects for the deviation from a pure Coulomb potential and $1-\epsilon$ is the correction for the finite size of the nucleus. $F_{rel}(Z\alpha)$ is a relativistic expression that contains the dependence on the atomic potential. Its explicit form is given in Eq.(6.3)[22]. The only relevant factors in this expression, however, are those that are dependent on α. This means that the only two factors that will cause a frequency shift due to variations in alpha are the $F_{rel}(\alpha Z)$ and the α^2 terms. The α^2, however,disappears when a ratio of two frequencies is considered. This leaves the $F_{rel}(\alpha Z)$ term as the only possible cause for a frequency drift. In order to magnify the variation of α in this type of experiment, one can take a natural log of this ratio as follows

$$\frac{d}{dt}\ln\left(\frac{A_1}{A_2}\right) = \alpha\frac{d}{d\alpha}\left[\ln(F_{rel}(\alpha Z_1)) - \ln(F_{rel}(\alpha Z_2))\right]\left(\frac{1}{\alpha}\frac{d\alpha}{dt}\right). \tag{6.2}$$

We notice here that this method will only be relevant for two atoms with different atomic numbers. The functional form of $F_{rel}(\alpha Z)$ is given by[22]

$$F_{rel}(\alpha Z) = 3[\lambda(4\lambda^2 - 1)]^{-1}, \tag{6.3}$$

where λ is defined as

$$\lambda = [1 - (\alpha Z)^2]^{1/2}. \tag{6.4}$$

Knowing the functional form of $F_{rel}(\alpha Z)$ the derivative in Eq.(6.2) can be taken to give:

$$\alpha \frac{d}{d\alpha} \ln(F_{rel}(\alpha Z) = L_d F_{rel}(\alpha Z), \tag{6.5}$$

where L_d is a function of λ. This allows for a simplification of Eq.(6.2) leading to the following expression

$$\frac{d}{dt} \ln\left(\frac{A_1}{A_2}\right) = (L_d F_{rel}(\alpha Z_1) - L_d F_{rel}(\alpha Z_2)) \left(\frac{1}{\alpha}\frac{d\alpha}{dt}\right). \tag{6.6}$$

This formula is used as a yes/no indicator. The ratio of two frequencies is periodically calculated for nearly a year. A yes response comes if the variation of the frequencies due to alpha changing is greater than the noise of the experiment.

An added feature of this method is that it allows for comparison of hyperfine transition frequencies in many different atoms. The atoms that are most often used are hydrogen, rubidium, cesium, and singly ionized mercury, because they are well defined systems that can be used as atomic clocks. The best comparison using the method in Eq.(6.6) comes from comparing the hyperfine transition frequencies of hydrogen and mercury because of the large difference in Z. A large difference of $Z_2 - Z_1$ maximizes the coefficients in front of $\dot{\alpha}/\alpha$ in Eq.(6.6). If this term is maximized, a small variation in α will lead to a large drift in the hyperfine frequencies and is hence much easier to detect. Using hydrogen and mercury in very accurate measurements, atomic clocks have measured no frequency drift and therefore no variation of α thus far. But they are only able to put an upper limit on the variation of α, namely $\dot{\alpha}/\alpha = 3.7 \times 10^{-14}/yr$. This constraint, however, is not competitive with the astrophysical measurement. Also, it may not necessarily be the best method for using atomic clocks as we will discuss in the next section.

6.1.2 Comparison of Two Transitions Between Two Nearly Degenerate States

The second method used by atomic clock physicists to measure the variability of the fine structure constants is to use an atom with two nearly degenerate levels[25]. The experiment is focused on a transition between these two nearly degenerate levels

on the one hand, and a third level on the other. This can be seen in figure 6.2 where A and B are the nearly degenerate states and G is the third state. If an atom with this behavior is simultaneously illuminated by two lasers able to stimulate transitions $A \leftrightarrow G$ and $B \leftrightarrow G$, a beat frequency will appear. This beat frequency will be much smaller than the two incident frequencies because the original transitions are nearly equal in energy. The measurement of this smaller beat frequency for the transition between $A \leftrightarrow B$ can be accomplished in a slightly different way, as seen in the work of Nguyen et al.[23].

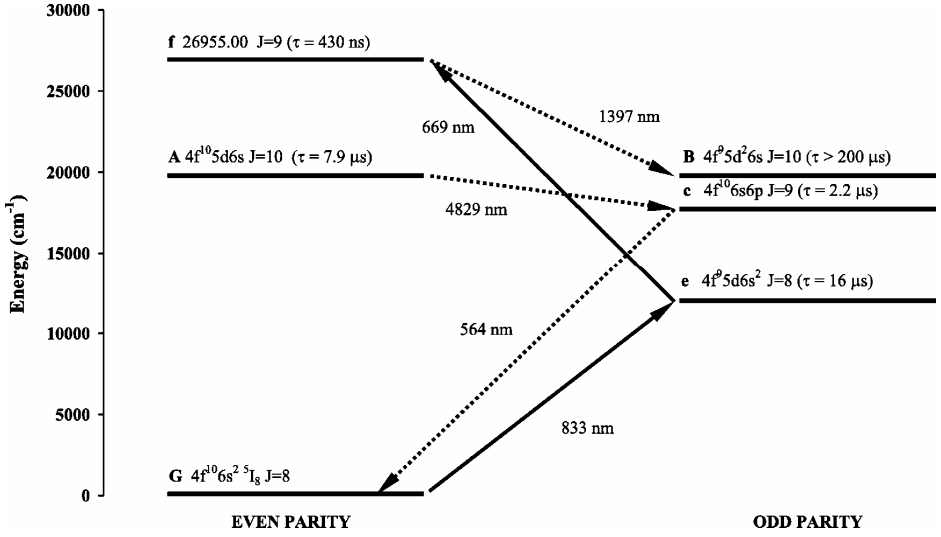

Figure 6.2: Transitions between two nearly degenerates labelled A and B(adapted from [23])

Because the beat frequency is several orders of magnitude smaller, it is easier to measure. Measurement of this beat frequency also allows for a more sensitive detection of the frequency drift between each of the two atomic transitions compared

to other atomic clock methods. The reason for this can be understood by considering two transitions which are equivalent in their first five(5) significant figures. For examples when two frequencies

$$\omega_1 = 565641934.3493.... \quad \omega_2 = 565643658.6465.... \tag{6.7}$$

are subtracted, a new frequency appears

$$\omega_2 - \omega_1 = 1724.2972... \quad . \tag{6.8}$$

A measurement of this difference with an accuracy of only eight(8) significant figures is able to detect a drift between frequencies of thirteen(13) decimal places. This means that the detection of the beat frequency of two nearly degenerate levels leads to a much more sensitive detection of the transitions frequencies drift. If the two nearly degenerate levels have different dependence on α, the beat frequency can be used as an indicator of α variability. Experimental methods measuring transitions between two nearly degenerate states are currently being performed in the hope of acquiring an accuracy of $\dot{\alpha}/\alpha \sim 10^{-18}/yr$[23]. This is three orders of magnitude better than the accuracy acquired by the astrophysicist and four orders of magnitude better than the two atom atomic clock method presented in Section 6.1.1. This level of accuracy would allow for possible verification of the astrophysicists' claims.

6.2 Discussion

Our discussion of atomic clock experiments leads to the conclusion that measurement of nearly degenerate energy levels is likely to give an added sensitivity to the physical behavior being measured. The reason for this is that it pushes the needed accuracy into decimal places that can be measured. It will be shown in chapter seven that this technique can be adapted for use in the Penning trap. It can be adapted using the electric field to force the spin flip frequency and the modified cyclotron frequency to be nearly equal.

Chapter 7

The Penning Trap

Geonium is an expression that was coined by Dehmelt[33]. Geonium is the name given to a single particle in a Penning trap. The term was used as the name for this state because geonium is in essence a bound state of an electron with the earth. The basis of our interest in the geonium trap is a comparison of two different frequencies, the spin precession and the cyclotron frequency. Classically the frequency is the inverse of the period which would corresponds to the time required to close an orbit. In quantum mechanics a frequency is directly proportional to the energy which corresponds to a transition between two different allowed energy levels. In the geonium experiment the classical and quantum frequencies are identical. In the geonium experiment two different frequencies are compared, the cyclotron frequency and the spin flip frequency. Because these frequencies depend on different dynamics but similar constants, a measurement of the anomalous magnetic moment is possible. Another advantage of using these two frequencies is that both of them can be measured in the same experiment, because both frequencies are characteristic of a constant magnetic field. In section 7.1 I present my derivation of classical and quantum solutions in the standard problem of the uniform magnetic field. In section 7.2 I present my derivation for the equivalent solution in the field of the Penning trap. I have thus checked independently the results originally derived by Sokolov and Pavlenko[10] and quoted in Van Dyck[32]. In section 7.3 I work out the effect of perturbing fields in a Penning trap. In section 7.4 I analyze the measurement of the anomaly frequency in a Penning trap, the time-dependent anomaly frequency in 7.5, and in section 7.6 I extend the analysis to include other particles.

7.1 The Uniform Magnetic Field

All measurable frequencies needed to determine the anomalous magnetic moment appear whenever an electron is placed in a uniform magnetic field. However, even if a uniform magnetic field were obtainable, it is very difficult to trap a particle in a uniform magnetic field. But the consideration of a particle in a uniform magnetic field will elucidate the essential features of this experiment. The two main features needed to measure the anomalous magnetic moment are a spin flip frequency and a cyclotron frequency, both of which are present in a uniform magnetic field.

7.1.1 Classical Trajectories

The cyclotron frequencies are obtained by solving Newton's equations for a charged particle exhibiting circular motion in a uniform magnetic field. The cyclotron frequency is the angular velocity at which the particle orbits in the magnetic field. The equation of motion for a charged particle in uniform magnetic field is

$$\frac{mv^2}{r} = qvB. \tag{7.1}$$

If the the angular velocity ω, defined as

$$v = \omega r \tag{7.2}$$

is introduced in Eq.(7.1) and then solved for, the following relationship is found

$$\omega = \frac{eB}{m} \equiv \omega_c, \tag{7.3}$$

where ω_c is the cyclotron frequency.

Although this is a purely classical calculation, it suggests that the energy of a particle orbiting in a uniform magnetic field is dependent on the same factors as in the spin precession case, except for the Landé factor. If this assumption holds true in the quantum case, then a measurement of these two frequencies will enable the calculation of the anomalous magnetic moment directly from observable quantities.

7.1.2 Quantum Levels

We will now tackle the same problem from a quantum mechanical point of view (the Landau problem). The Landau problem consists in solving the Schrödinger equation for a particle in a uniform magnetic field. The differential equation to be solved takes the form

$$\frac{1}{2m}(-i\hbar\vec{\nabla} - \frac{e}{c}\vec{A})^2\psi = E\psi. \tag{7.4}$$

Here $\vec{A}$ is the magnetic vector potential which is related to the magnetic field $\vec{B}$ in the usual way

$$\vec{B} = \vec{\nabla} \times \vec{A}. \tag{7.5}$$

Because of the gauge freedom of electromagnetism an ambiguity arises. Which gauge should be used, and does the gauge affect the wave function and energies of the solution? Another choice that arises is that of the coordinates. Because the symmetry of the geonium trap is cylindrical, I have chosen to solve this problem in cylindrical coordinates (ρ, ϕ, z). The problem is solvable in Cartesian coordinates with a different choice of gauge [30]. I have chosen the gauge where the vector potential is given as

$$\vec{A} = \frac{B\rho}{2}\hat{\phi}, \tag{7.6}$$

where B is the magnitude of $\vec{B}$.

Because the potential is only a function of the radial coordinate ρ, the equation can be shown to be separable in cylindrical coordinates. The solution is assumed to be of the form

$$\Psi(\rho, \phi\, z) = R(\rho)\exp(ikz)\exp(il\phi), \tag{7.7}$$

where k and l are constants to be determined later. If the wave function is assumed to be of this form, the partial differential equation is transformed into the following ordinary differential equation:

$$R''(\rho) + \frac{1}{\rho}R'(\rho) + (\frac{2mE}{\hbar^2} - k^2 + 2l\gamma - \gamma^2\rho^2 - \frac{l^2}{\rho^2})R(\rho) = 0 \tag{7.8}$$

where the constant gamma contains the strength of the magnetic field

$$\gamma = \frac{eB}{\hbar c}. \tag{7.9}$$

It can be shown that this differential equation has singular points at the origin and at infinity. In order to get a differential equation that is solvable, the singular behavior needs to be removed. The singular behavior of the solution is removed by first making a change of variable

$$r = \gamma\rho^2. \tag{7.10}$$

After this change of variables is performed, the following substitution, inspired by the singular behavior of the equation, is made

$$R(r) = \exp(-\frac{r}{2})r^{\frac{l}{2}}Q(r). \tag{7.11}$$

This transforms the differential equation into a well-known expression

$$rQ''(r) + (l - r + 1)Q'(r) + nQ(r) = 0, \tag{7.12}$$

where the constant n combines physical parameters, including the still undetermined energy E of the system, as follows

$$n = \frac{mE}{2\hbar^2\gamma} - \frac{k^2}{4\gamma} - \frac{2l+1}{2}. \tag{7.13}$$

The solution to this differential equation is the well-known associated Laguerre polynomials L_n^l. In order for the solution to be finite, the series must terminate, forcing the constants n and l to be integers. The radial solution and the energy values take the form

$$R(\rho) = \exp(-\gamma\rho^2)(\gamma\rho^2)^{\frac{l}{2}}L_n^l(\gamma\rho^2), \tag{7.14}$$

$$E = (2n + l + 1)\hbar\omega_c, \tag{7.15}$$

where n is the radial quantum number and l is the azimuthal quantum number, which can be positive or negative. Thus we see that the quantum frequency for a transition between two adjacent energy levels is the same as that of the classical problem in analogy to what happens in the case of the simple harmonic oscillator.

7.1.3 Classical Precession

We now consider a particle with a magnetic moment in a uniform magnetic field. The classical problem is to solve the torque equation relating the torque $\vec{\tau}$ to a magnetic moment and an external magnetic field. The equation of motion is

$$\vec{\tau} = \vec{\mu} \times \vec{B} \tag{7.16}$$

The magnetic moment of a particle of charge e and mass m is related to the angular momentum $\vec{L}$ of the particle by the gyromagnetic ratio γ such that

$$\vec{L} = \frac{\vec{\mu}}{\gamma}, \tag{7.17}$$

and

$$\gamma = \frac{ge}{2m}. \tag{7.18}$$

Torque is the time derivative of angular moment

$$\vec{\tau} = \frac{d\vec{L}}{dt}. \tag{7.19}$$

Combining Eq.(7.16)-(7.17), and Eq.(7.19) leads to

$$\frac{d\vec{\mu}}{dt} = \gamma\vec{\mu} \times \vec{B}. \tag{7.20}$$

This differential equation has an exact solution for a uniform magnetic field

$$\vec{B} = B_0\hat{z}. \tag{7.21}$$

The solution for this field configuration is

$$\vec{\mu} = A\left[\cos(\gamma B_0 t + \delta)\hat{x} + \sin(\gamma B_0 t + \delta)\hat{y} + C\hat{z}\right], \tag{7.22}$$

where δ and C are constants of integration related to initial values. From examining the solution, it is seen that the frequency at which the spin precesses around the magnetic field is

$$\omega_0 = \gamma B_0 = \frac{geB_0}{2m}. \tag{7.23}$$

We will see that this is the same as the spin flip frequency for an electron in a uniform magnetic field.

7.1.4 Spin Flip

The spin precession frequency is obtained by considering the Hamiltonian, (H), of the form

$$H = -\vec{\mu} \cdot \vec{B} \tag{7.24}$$

where the magnetic moment $\vec{\mu}$ and the magnetic field

$\vec{B}$ are defined as

$$\vec{\mu} = -g\frac{e}{2m}\vec{S} \tag{7.25}$$

$$\vec{B} = B_0\hat{z} \tag{7.26}$$

In the following equations e is the charge of an electron, g is the Landé factor, m is the mass of an electron and $\vec{S}$ is the spin vector. Substituting Eq. (7.25)-(7.26) into Eq. (7.24) gives an eigenvalue equation

$$\mu_z B_z X = g\frac{eB_0}{2m}S_z X = \lambda X, \tag{7.27}$$

where

$$S_z = \frac{\hbar}{2}\sigma_z, \tag{7.28}$$

and σ_z is a Pauli matrix. The solution of this eigenvalue problem is

$$X_+ = \begin{pmatrix} 1 \\ 0 \end{pmatrix}, \tag{7.29}$$

$$X_- = \begin{pmatrix} 0 \\ 1 \end{pmatrix}, \tag{7.30}$$

with energy eigenvalues of

$$\lambda = E_\pm = \frac{\pm\hbar\omega_0}{2}, \tag{7.31}$$

and where ω_0 is the spin precession frequency defined as

$$\omega_0 = \frac{geB_0}{2m}. \tag{7.32}$$

As is seen from the eigenvalues of this equation, the energies of these states are dependent on the value of the Landé factor, g. This means that g can be obtained by a measurement of the energies of spin precession. However, without a comparison there is no way to get directly at g without relying on other experimental data, which increases the error. By considering the cyclotron frequency of a given particle and its accompanying spin flip frequency, the Landé factor is found as the ratio

$$g = \frac{2\omega_0}{\omega_c}. \tag{7.33}$$

If a particle could be contained by a uniform magnetic field while the measurements of ω_0 and ω_c are made, the problem of measuring the anomalous magnetic moment could be solved. However, this is impossible in the present configuration. In order to contain a particle, an electric field must be added to confine the particle in the axial direction. According to Maxwell's equations the divergence of the electric field must be zero in a region with no charge. In order to keep the divergence of the electric field zero, in addition to the axial component of the electric field there will be a radial component. This added radial electric field will cause a shift in the cyclotron frequency from that of the pure magnetic field. To obtain an accurate calculation of the anomalous magnetic moment, a relation between the measured cyclotron frequency and the actual cyclotron frequency must be found.

7.2 Physical Quantities in the Penning Trap

The trap that is used in the geonium experiment is the Penning trap. A Penning trap is composed of a uniform magnetic field that is superimposed on an electric field that is predominantly a quadrupole field. The quadrupole field is obtained by precision machining of the electrodes in the shape of hyperbola. If this is done the equation for the potential in the Penning trap is

$$\Phi(r, z) = U_0 \frac{r^2 - 2z^2}{4Z_0^2}, \tag{7.34}$$

where U_0 is the potential on the electrode and Z_0 is a measure of the size of the trap. A simple picture of the trap can be seen in figure 7.1.

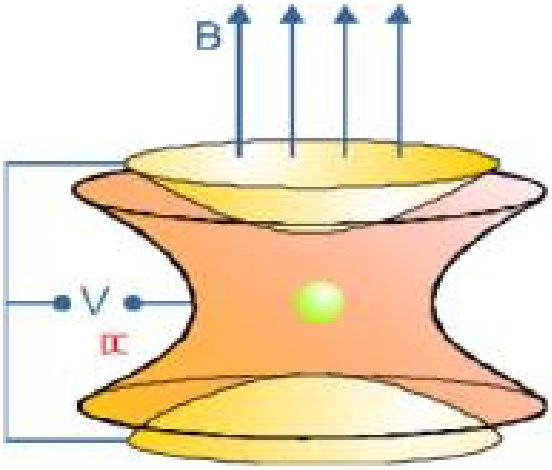

Figure 7.1: Lay out of the Penning trap (adapted from [26])

Due to the complexity added by the electric field, the particle will now exhibit a more complicated motion. Instead of a simple circular orbit the particle will perform simple harmonic motion in the axial direction and the previously simple circular orbits will now become the superposition of two circular orbits of different sizes. The trajectory of the particle can be seen in figure 7.2.

7.2.1 Classical Frequencies in the Trap

Because the divergence of the electric field must be zero in a region with no charges, the electric field must have a radial component. This is seen to be true when the electric field is calculated from the potential

$$e\vec{E} = -\vec{\nabla}\Phi = \frac{-U_0}{2Z_0^2}[-r\hat{r} + 2z\hat{z}]. \tag{7.35}$$

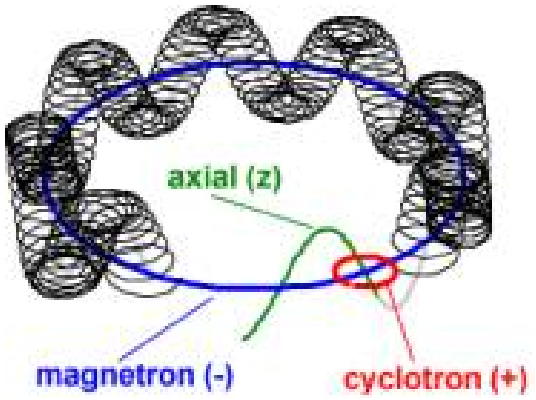

Figure 7.2: Classical trajectories in the Penning trap (adapted from [26])

This radial portion of the electric field alters the simple form of Newton's equations for a particle in a uniform magnetic field. The added forces due to the superimposed electric field are

$$F_r = ma_r = e\frac{U_0}{2Z_0^2}r = m\omega_r^2 r, \tag{7.36}$$

$$F_z = ma_z = -\frac{U_0}{Z_0^2}z = -m\omega_z^2 z, \tag{7.37}$$

$$\omega_r^2 = \frac{\omega_z^2}{2} = \frac{U_0}{Z_0 m}. \tag{7.38}$$

Newton's equation for the radial motion of a particle in a Penning trap becomes

$$qvB - \frac{m_0\omega_z^2 r}{2} = \frac{m_0 v^2}{r}. \tag{7.39}$$

If constants are collected and defined the equation for the frequency ω becomes

$$2\omega(\omega_c - \omega) = \omega_z^2, \tag{7.40}$$

with the following definitions

$$\omega = \frac{v}{r}, \tag{7.41}$$

$$\omega_c = \frac{eB}{m}. \tag{7.42}$$

The frequency ω in Eq. (7.40) can now be solved for. As is clear from Eq. (7.40) the radial electric field has changed the frequency of oscillation. Because the equation for the frequency is quadratic there will be two different frequencies. The two allowed orbital frequencies are

$$\omega = \frac{\omega_c \pm \sqrt{\omega_c^2 - 2\omega_z^2}}{2}, \tag{7.43}$$

which is approximately equal to

$$\omega = \omega_c' \approx \omega_c - \delta_e, \tag{7.44}$$

$$\omega = \omega_m = \delta_e \approx \frac{\omega_z^2}{2\omega_c}. \tag{7.45}$$

These two new frequencies are defined as the modified cyclotron frequency ω_c' and the magnetron frequency ω_m. The cyclotron frequency is the frequency at which the particle orbits the magnetic fields and the magnetron frequency is the frequency at which the center of the cyclotron orbit rotates about the center of the trap. An illustration of this is shown is figure 7.3.

An advantage of using the Penning trap is that the frequencies of a perfectly aligned trap, ω_c', ω_m, and δ_e, are independent of the particle location in the trap. This is a significant advantage because it creates a relation between ω_z and ω_m that can be used to identify trap imperfections.

7.2.2 Classical Trajectories in the Trap

Using the Lorentz force equation the equations of motion for the particle in the trap can be found. The equations reduce to[32]

$$\ddot{x} - \frac{\omega_z^2}{2}x + \omega_c\dot{y} = 0, \tag{7.46}$$

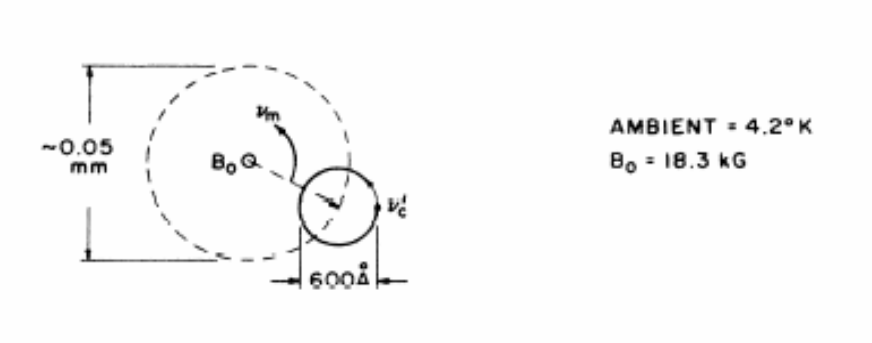

Figure 7.3: Comparison of cyclotron and magnetron radii (adapted from [32])

$$\ddot{y} - \frac{\omega_z^2}{2} y - \omega_c \dot{x} = 0, \tag{7.47}$$

$$\ddot{z} + \frac{\omega_z^2}{2} \dot{z} = 0. \tag{7.48}$$

The z equation describes a one-dimensional simple harmonic oscillator and is easily solved. The solution to the z equation is harmonic. In order to solve the x and y equations it is easiest to complexify the variables as follows

$$\xi = x + iy. \tag{7.49}$$

If this substitution is made, the differential equations for x and y can be combined into one differential equation of the form

$$\ddot{\xi} - \omega_c \dot{\xi} - i\frac{\omega_z^2}{2} \dot{\xi} = 0. \tag{7.50}$$

This equation is easily solved

$$\xi = r_c \exp(i\omega_c' t + \delta_1) + r_m \exp(i\omega_m t + \delta_2) \tag{7.51}$$

where ω_c and ω_m are as defined in Eq.'s(7.44)-(7.45) and r_c, r_m, δ_1, and δ_2 are determined from the initial conditions.

7.2.3 Quantum Solutions of the Penning Trap

The quantum solution is obtained by solving Schrödinger's equation in the following form[10]

$$\frac{1}{2m}(-i\hbar\vec{\nabla} - \frac{e}{c}\vec{A})^2 \psi(r,\theta,\phi) + \Phi(r)\psi(r,\theta,\phi) = E\psi(r,\theta,\phi), \tag{7.52}$$

where the electric and magnetic potential are defined as follows

$$\Phi(r,z) = e^2 a \frac{r^2 - 2z^2}{2}, \tag{7.53}$$

$$\vec{A} = \frac{Br}{2}\hat{\phi}, \tag{7.54}$$

and

$$a = \frac{U_0}{2Z_0^2}. \tag{7.55}$$

Because the symmetry of the trap is known, a good guess for the solution (which turns out to be correct) is

$$\Psi(\rho, \phi\, z) = R(\rho)u(z)\exp(il\phi), \tag{7.56}$$

if the energy is defined as

$$E = E_1 + E_2. \tag{7.57}$$

After separation the remaining two differential equations take the form

$$R''(\rho) + \frac{1}{\rho}R'(\rho) + (\frac{2mE_1}{\hbar^2} - 2l\gamma - \gamma_1^2\rho^2 - \frac{l^2}{\rho^2})R(\rho) = 0, \tag{7.58}$$

$$u''(z) + (\frac{2m_0E_2}{\hbar^2} - \gamma_2^2 z^2)u(z) = 0. \tag{7.59}$$

The radial equation is solved by first making a change of variables

$$\rho = \gamma_1 r^2. \tag{7.60}$$

The differential equation then takes the form

$$R''(\rho) + \frac{1}{\rho}R'(\rho) + (\frac{mE_1}{2\hbar^2\gamma_1} - \frac{\gamma l}{2\gamma_1\rho} - \frac{l^2}{4\rho^2} - \frac{1}{4})R(\rho) = 0. \tag{7.61}$$

In order to remove the singular behavior at the origin and at infinity the following substitution is made

$$R(r) = \exp\left(-\frac{\rho}{2}\right)\rho^{\frac{l}{2}}Q(\rho). \tag{7.62}$$

Notice the similarity to the pure magnetic field Eq.(7.11). The new differential equation for $Q(\rho)$ simplifies to

$$\rho Q''(\rho) + (l - \rho + 1)Q'(\rho) + nQ(\rho) = 0, \tag{7.63}$$

where l is the azimuthal quantum number and n is defined as

$$n = \frac{mE_1}{2\hbar^2\gamma_1} - \frac{l+1}{2} - \frac{\gamma l}{2\gamma_1}. \tag{7.64}$$

The solution to this differential equation is

$$R(r) = \exp(-\frac{\gamma_1 r^2}{2})(\gamma_1 r^2)^{\frac{l}{2}} L_n^l(\gamma_1 r^2), \tag{7.65}$$

where $L_n^l(\gamma_1 r)$ are the associated Laguerre polynomials.

The axial equation is solved by first removing the singular behavior at infinity by making the following substitution

$$U(z) = \exp\left(\frac{-\gamma_2 z^2}{2}\right) Z(z), \tag{7.66}$$

followed by a change of variable of

$$\zeta = \sqrt{\gamma_2} z \tag{7.67}$$

the differential equation then takes the following form

$$Z'' - 2\zeta Z' + 2nZ = 0, \tag{7.68}$$

with the quantum number k defined as

$$k = \frac{mE_2}{\hbar^2\gamma_2} - \frac{1}{2}. \tag{7.69}$$

The solutions are the Hermite polynomials and the complete axial solution is

$$U(z) = \exp\left(\frac{-\gamma_2 z^2}{2}\right) H_k(\sqrt{\gamma_2} z). \tag{7.70}$$

This solution requires that the quantum number n be an integer for the solution not to diverge.

The total energy due to the radial motion and the axial motion is as follows

$$E_n^{(0)} = \hbar\left(\omega_c'(s+\frac{1}{2}) - \omega_m(n+\frac{1}{2}) + \omega_z(k+\frac{1}{2})\right), \tag{7.71}$$

where $s = n + l$. If the γ factors in the frequencies are replaced by their physical parameters the frequencies can be defined as follows

$$\omega_c' = \frac{\omega_c}{2} + \frac{\omega_c}{2}\sqrt{1 - \frac{4amc^2}{B^2}}, \tag{7.72}$$

$$\omega_m = \frac{\omega_c}{2} - \frac{\omega_c}{2}\sqrt{1 - \frac{4amc^2}{B^2}}, \tag{7.73}$$

and

$$\omega_z = \sqrt{\frac{2e^2a}{m}}. \tag{7.74}$$

As is seen from this discussion, the frequencies of the quantum solution are the same as the frequencies from the classical solutions. However in the quantum case, the frequencies represent an energy transition and not an actual frequency. Now that the solutions have been found for a particle in the Penning trap, consideration must be given on how to make a measurement in the trap. In particular the effect of stray fields must be considered in order to know the accuracy of measurements in the trap.

7.2.4 Spin Flip in the Penning Trap

Because the Penning trap has a uniform axial magnetic field, the spin contribution can be easily accounted for. An axial magnetic field leads to a σ_z contribution in the Hamiltonian. Because σ_z is a diagonal matrix, the up and down component will never mix. This means that the spinor solution previously found in section (7.1.4) will still work. This leads to an equation for the total energy

$$E_n^{(0)} = \hbar\left(\omega_c'(s + \frac{1}{2}) - \omega_m(n + \frac{1}{2}) + \omega_z(k + \frac{1}{2}) + m\omega_s\right), \tag{7.75}$$

where m is the spin quantum number.

7.3 Perturbation of the Penning Trap

If a good measurement of the variability of the fine structure constant is to be made, the Penning trap needs to be insensitive to extraneous magnetic fields. In order to determine the trap's sensitivity to these extraneous magnetic fields, they will be treated as a perturbation of a perfect trap.

7.3.1 Perturbations Under a Constant Magnetic Field

The total magnetic field in the trap can be decomposed as a sum of the unperturbed field plus a small perturbation. The magnetic field can be defined in terms of a vector potential $\vec{A}$ in the following way

$$\vec{B} = \vec{\nabla} \times \vec{A}. \tag{7.76}$$

Because this is a linear relation the magnetic vector potential can also be decomposed into the unperturbed potential plus a small perturbation

$$\vec{A} \rightarrow \vec{A} + g\vec{A'}. \tag{7.77}$$

The Schrödinger equation for the new system is only slightly modified to give

$$(-i\hbar\vec{\nabla} - \frac{e}{c}(\vec{A} + g\vec{A'}))^2\Psi + V\Psi = E\Psi. \tag{7.78}$$

This can be rewritten as

$$\begin{aligned} &(-i\hbar\vec{\nabla} - \frac{e}{c}\vec{A})^2\Psi + V\Psi \\ &-g\frac{e}{c}[(-i\hbar\vec{\nabla} - \frac{e}{c}\vec{A}) \cdot \vec{A'} + \vec{A'} \cdot (-i\hbar\nabla - \frac{e}{c}\vec{A})] + g^2A'^2 = E\Psi. \end{aligned} \tag{7.79}$$

The wave function and the energy are then expanded as power series in the parameter g in the following way

$$E_n = E_n^{(0)} + gE_n^{(1)}...., \tag{7.80}$$

$$\Psi_n = \Psi_n^{(0)} + g\Psi_n^{(1)}...., \tag{7.81}$$

which are then substituted into Eq.(7.79). If only the terms that are zeroth order in g are kept, the resultant equation is

$$(-i\hbar\vec{\nabla} - \frac{e}{c}\vec{A})^2\Psi_n^{(0)} + V\Psi_n^{(0)} = E_n^{(0)}\Psi_n^{(0)}. \tag{7.82}$$

This is the equation for the unperturbed Penning trap, justifying the assumption that the solution can be written as a perturbation of the unperturbed trap solution. If the terms that are first order in g are kept, the following relationship is found

$$(-i\hbar\vec{\nabla} - \frac{e}{c}\vec{A})^2\Psi_n^{(1)} + V\Psi_n^{(1)} - \frac{e}{c}\{(-i\hbar\vec{\nabla} - \frac{e}{c}\vec{A}), \vec{A}'\}\Psi_n^{(0)} = E_n^{(1)}\Psi_n^{(0)} + E_n^{(0)}\Psi_n^{(1)}, \tag{7.83}$$

where the curly bracket denotes an anticommutator ($\{A, B\} = AB + BA$).

If the previous equation is projected onto the unperturbed wave function, the equation becomes

$$\begin{aligned}&\langle\Psi_n^{(0)}|(-i\hbar\vec{\nabla} - \frac{e}{c}\vec{A})^2|\Psi_n^{(1)}\rangle + \langle\Psi_n^{(0)}|V|\Psi_n^{(1)}\rangle \\ &-\langle\Psi_n^{(0)}|\{(-i\hbar\vec{\nabla} - \frac{e}{c}\vec{A}), \frac{e}{c}\vec{A}'\}|\Psi_n^{(0)}\rangle = E_n^{(1)}\langle\Psi_n^{(0)}|\Psi_n^{(0)}\rangle + E_n^{(0)}\langle\Psi_n^{(0)}|\Psi_n^{(1)}\rangle.\end{aligned} \tag{7.84}$$

Using the fact that the unperturbed Hamiltonian is hermitian and can operate unchanged to the left, the equation simplifies to

$$E_n^{(0)}\langle\Psi_n^{(0)}|\Psi_n^{(1)}\rangle - \langle\Psi_n^{(0)}|\{(-i\hbar\vec{\nabla} - \frac{e}{c}\vec{A}), \frac{e}{c}\vec{A}'\}|\Psi_n^{(0)}\rangle = E_n^{(1)} + E_n^{(0)}\langle\Psi_n^{(0)}|\Psi_n^{(1)}\rangle. \tag{7.85}$$

This leads to an expression for the first order energy

$$-\langle\Psi_n^{(0)}|\{(-i\hbar\vec{\nabla} - \frac{e}{c}\vec{A}), \frac{e}{c}\vec{A}'\}|\Psi_n^{(0)}\rangle = E_n^{(1)}. \tag{7.86}$$

The expression for the unperturbed energy given by Eq.(7.71) as

$$E_n^{(0)} = \hbar\left[\omega_c'(n + \frac{1}{2}) - \omega_m(s + \frac{1}{2}) + \omega_s(k + \frac{1}{2})\right], \tag{7.87}$$

which is clearly not degenerate since ω_c', ω_m and ω_s given in Eq.(7.106), (7.73), and (7.74) are not commensurate. This means that non-degenerate perturbation theory can be used in this problem.

Because the trap is small, a constant perturbing field should be a good approximation to most fields. The solution of the perfect trap has a constant magnetic field in the axial direction therefore a perturbation in this direction can be accounted for by substituting $B \rightarrow B + gB'$ into the unperturbed solution. However, a magnetic field in a direction perpendicular to the axis needs to be treated as a perturbation. A vector potential for a constant magnetic field $(B_x, B_y, 0)$ in the plane perpendicular to the axis is

$$A'_z = B'_x y - B'_y x. \tag{7.88}$$

When written in cylindrical coordinates this potential becomes

$$A'_z = \rho(B'_x \sin(\phi) - B'_y \cos(\phi)). \tag{7.89}$$

In order to evaluate the first correction to the energy, the anti-commutator in Eq.(7.86) must be expanded and simplified. When expanded the anti-commutator in Eq.(7.86) becomes

$$-2(\frac{e}{c})^2 \vec{A} \cdot \vec{A'} - i\frac{e}{c}\hbar((\vec{\nabla} \cdot \vec{A'}) + 2\vec{A'} \cdot \vec{\nabla}). \tag{7.90}$$

This expression can be simplified using the fact that the perturbing vector potential is in the $\hat{z}$ direction, the unperturbed vector potential is in the $\hat{\phi}$ direction and the perturbing potential is divergenceless. This simplification gives

$$\frac{e}{c}\{(-i\hbar\vec{\nabla} - \frac{e}{c}\vec{A}), \cdot\vec{A'}\} = -i2\hbar A'_z \frac{e}{c}\frac{\partial}{\partial z}. \tag{7.91}$$

This allows the first order corrections to the energy to be written as

$$E_n^{(1)} = \langle \Psi_n^{(0)} | i2\hbar A'_z \frac{e}{c}\frac{\partial}{\partial z} | \Psi_n^{(0)} \rangle. \tag{7.92}$$

If A_z is substituted and the ϕ integral is shown explicitly, the expression for the energy can be written as

$$E_n^{(1)} = -2\frac{e}{c}\int_0^{2\pi} (B'_x \sin(\phi) - B'_y \cos(\phi)) d\phi \langle \Psi_n^{(0)}(\rho, z) | \rho i\hbar \frac{\partial}{\partial z} | \Psi_n^{(0)}(\rho, z) \rangle. \tag{7.93}$$

Each of these ϕ integrals is separately zero, thus leading to a vanishing energy correction

$$E_n^{(1)} = 0. \tag{7.94}$$

The next and first nonvanishing contribution from the perturbative field is of order g^2. This shows that the Penning trap has a low sensitivity to extraneous magnetic fields in the direction perpendicular to the axis.

7.3.2 Perturbation Under z-independent Magnetic Fields

The previous results can be shown to be valid for any magnetic field that can be obtained from a magnetic vector potential in the z direction that has no z dependence. Every magnetic field perpendicular to the axial direction can be written in terms of a vector potential of this form. Substituting this vector potential into Eq.(7.86)

$$\{(-i\hbar\vec{\nabla} - \frac{e}{c}\vec{A}), \vec{A'}\} = -2\frac{e}{c}\vec{A}\cdot\vec{A'} - i\hbar((\vec{\nabla}\cdot\vec{A'}) + 2\vec{A'}\cdot\vec{\nabla}), \tag{7.95}$$

leads to

$$\{(-i\hbar\vec{\nabla} - \frac{e}{c}\vec{A}), \vec{A'}\} = -i2\hbar A'_z(\rho,\phi)\frac{\partial}{\partial z}. \tag{7.96}$$

This time the z dependent portion of the wave function is shown explicitly in the expansion for the lowest order correction

$$\begin{aligned} E_n^{(1)} = -\frac{e}{c}\int_0^\infty dz H_n(\sqrt{\gamma_1}z)\exp(\frac{-\gamma_1 z^2}{2})\frac{\partial}{\partial z}H_n(\sqrt{\gamma_1}z)\exp(\frac{-\gamma_1 z^2}{2}) \\ \times\frac{e}{c}\langle\Psi_n^{(0)}(\rho,\phi)|i2\hbar A'_z(\rho,\phi))|\Psi_n^{(0)}(\rho,\phi)\rangle, \end{aligned} \tag{7.97}$$

where $H_n(\sqrt{\gamma_1}z)$ are the Hermite polynomials. If the derivative is expanded, the integral expression becomes

$$\int_0^\infty dz H_n(\sqrt{\gamma_1}z)\exp(\frac{-\gamma_1 z^2}{2}) \tag{7.98}$$
$$\times(nH_{n-1}(\sqrt{\gamma_1}z)\exp(\frac{-\gamma_1 z^2}{2}) - z\gamma_1 H_n(\sqrt{\gamma_1}z)\exp(\frac{-\gamma_1 z^2}{2})dz$$

The first term in this expression is zero due to the orthogonality of the Hermite polynomials. The second term is zero because Hermite polynomials have either even or odd parity and z has odd parity which means that the integral is equal to its negative under coordinate reversal and therefore zero. This result can also be found in Merzbacher[12] Eq.(5.32). The first order correction to the energy vanishes

$$E_n^{(1)} = 0. \tag{7.99}$$

The insensitivity of the trap remains even in this case. This means that experimentalists can be confident that their measurements are unaffected by stray magnetic fields.

7.4 Measurements in the Penning Trap

The high stability of the Penning trap has allowed experimentalists to contain a charged particle for up to several months and this helped in making high precision measurements using the Penning trap.

Although the Penning trap is an excellent method for confining a particle it does not readily allow for measurement. However, if a small inhomogeneous magnetic field is added, the trap is given the flexibility necessary for high precision measurements. This small magnetic field is added by placing a small circular nickel wire which is coaxial with the trap and centered on the z axis halfway between the two electrodes. The power of this small magnetic field is that it can cause spin flip, and at the same time, it provides a method to detect this spin flip. The magnetic field that allows this to be done is of the form ($\beta \ll B_0$)

$$\vec{B} = -\beta z x\hat{x} - \beta z y\hat{y} + \beta(z^2 - \rho^2/2)\hat{z}. \tag{7.100}$$

The inclusion of this magnetic field does two things. First, it creates a spin dependence in the axial frequency ω_z. To see why this happens, first consider the potential energy due to the magnetic field in Eq.(7.100). The potential energy due to this field that contributes to the axial oscillation is (on axis, $x = 0$, $y = 0$)

$$U'_m = -\vec{\mu} \cdot \vec{B} = -\mu_z \beta z^2. \tag{7.101}$$

The force due to this magnetic field is

$$F_m^z = -\frac{\partial U'_m}{\partial z} = 2\mu_z \beta z. \tag{7.102}$$

The equation for the total force on a particle in the trap must be modified to include the new term

$$F_z = ma_z = -m\omega_{z_0}^2 z + 2\mu_z \beta z. \tag{7.103}$$

The new frequency of the axial motion is

$$\omega_z^2 = \omega_{z_0}^2 - \frac{2\mu_z \beta}{m}. \tag{7.104}$$

The ω_z is now dependent on the orientation of the spin. Because ω_z is spin dependent, experimentalists are able to determine the spin orientation from measuring ω_z. Because ω_z is three orders of magnitude smaller than the other frequencies of the trap, it can be measured by detecting an image charge current. This allows for detection of the spin without greatly disturbing the system.

The other feature of the added magnetic field is its ability to force spin flip. This is accomplished by oscillating the magnetic field of the nickel wire at the frequency ω'_a which is defined as

$$\omega'_a = \omega_s - \omega'_c. \tag{7.105}$$

The oscillating field can be decomposed into two different fields precessing in the opposite sense as seen in figure 7.4. From this point of view the particle will see a field that is precessing at $\omega_s = \omega'_a + \omega'_c$. This means that the particle sees a magnetic

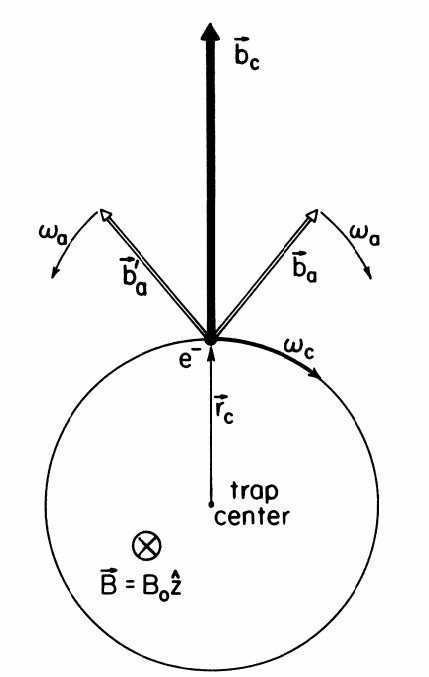

Figure 7.4: The field of the nickel wire (adapted from [32])

field that is at the spin flip frequency. A particle that is modulated at the spin flip frequency will have maximal oscillation between its two spin states. This means that when an experimentalist is locked into the correct ω'_a the system will have a maximal number of spin flips. Experimentalists can determine that the frequency they are modulating the magnetic field at, is ω'_a, by monitoring the axial frequency. Under this technique the axial frequency is only used to determine the number of spin flips so as to determine when the maximal rate of spin flip occurs. Although this has been outlined for the trap, this is true for the unprimed frequencies that are found in a uniform magnetic field as well. Figure 7.4 illustrates the case of a uniform magnetic field, however, the diagram would be identical for the Penning trap.

7.5 Time Dependent Alpha Measurements in a Penning Trap

The geonium experiment has built into it a method for measuring the time dependence of the fine structure constant. This method is manifest in the measurement of ω_a. Because ω_a is the difference between ω_s and ω_c it should drift as α drifts. The reason for this is that the spin flip frequency, ω_s, is dependent on the Landé factor, g. The Landé factor is related to the anomalous magnetic moment, which is related to α through QED. On the other hand the cyclotron frequency, ω_c, is independent of α. It is a measure of the response of a charged particle to a magnetic field and is independent of its spin. This means that the frequency ω_a is highly sensitive to changes in ω_s. Because $\omega_a \approx 10^{-3}\omega_s$, a drift in ω_a corresponds to a drift in ω_s of three more significant figures than are present in ω_a.

At first glance it may appear that the addition of the electric field in the trap allows for nearly infinite accuracy on the detection of the variability of the fine structure constant. A first thought would be to use the electric field to push ω_c' and ω_s even closer, and hence allowing for even more sensitivity on ω_s. However, things are not that simple. If the solution of the frequencies of the trap are examined, it is found that there is a minimal difference between ω_s and ω_c' for a particle confined in a trap. The allowed cyclotron frequencies in the trap comes from the following relation

$$\omega_c' = \frac{\omega_c \pm \omega_c\sqrt{1 - \frac{4amc^2}{B^2}}}{2}, \tag{7.106}$$

where a is a measure of the magnitude of the electric field, B is a measure of the magnitude of the magnetic field, m is the mass of an electron, c is the speed of light and ω_c is the cyclotron frequency if the electric field were zero. In order to keep the particle bound there are two constraints on a. First, a must be small enough so that the term in the square root in Eq.(7.106) is real. If the radical becomes imaginary the particle will be able to escape in the radial direction, because the force of the radial electric field is greater than the radial force due to the magnetic field. This means that the particle will escape in the $\hat{\rho}$ direction. The other constraint is $a > 0$. The reason that a has to be greater than zero is to retain confinement in the $\hat{z}$ direction.

If a changes signs and becomes negative, the electric field, which was confining the particle in the $\hat{z}$ direction, becomes a nonconfining field and the particle is free to leave the trap. However, it should be noted that the radial magnetic confinement is now reinforced by the electric field.

Because of the constraints necessary for confinement, the maximal value for the cyclotron frequency in the trap occurs when the radical in Eq. (7.106) is equal to one. This occurs when $a = 0$, leading to a maximum cyclotron frequency equal to the cyclotron frequency without the electric field. Thus the frequency ω_a' can never be smaller than $a_e\omega_s$, where a_e is the anomalous magnetic moment. Therefore, the maximal accuracy gain on ω_s through measurement of ω_a is only three orders of magnitude. Because experimentalists can obtain a drift sensitivity on $\delta\omega_a/\omega_a$ of approximately 1 ppb, a sensitivity of 1 ppt can be obtained on the drift of ω_s. This, however, is not competitive with atomic clock measurements.

7.6 Possible Extensions of the Resonance Measurement

7.6.1 Smaller Anomaly Frequency

We determined previously in this chapter that a measurement of the anomaly frequency in the trap could not be smaller than $a_e\omega_c$. The reason for this is that a trapped particle can never have its cyclotron frequency and spin flip frequency closer than $a_e\omega_c$. This can be seen by reexamining Eq. (7.106)

$$\omega_c' = \frac{\omega_c}{2} + \frac{\omega_c}{2}\sqrt{1 - \frac{4amc^2}{B^2}}. \tag{7.107}$$

The maximum value for ω_c' is obtained when the radical reduces to one. This corresponds to a zero electric field solution. Then Eq. (7.107) reduces to the cyclotron frequency of a particle in a uniform magnetic field which is

$$\omega_c = \frac{eB}{m}. \tag{7.108}$$

The difference between cyclotron frequency in the absence of an electric field and the spin flip frequency is

$$\omega_s - \omega_c = \frac{geB}{2m} - \frac{eB}{m} = \frac{g-2}{2}\frac{eB}{m} = a_e\omega_c, \tag{7.109}$$

as previously stated. However, this constraint is not present on a free particle. If a in equation 7.107 is taken to be $a < 0$, which corresponds to reversing the electric field, the spin flip frequency and the cyclotron frequency could be made equal. The problem with doing this is that the particle is free to escape in the axial direction and thus measurement is not possible using the method outlined by Dehmelt. But if a measurement of the anomaly frequency of a single significant figure were possible, it would yield infinite accuracy on the drift of the spin flip frequency. This would make it a competitive method for determining the variability of α.

7.6.2 Systems With Landé Factors Less Than 2 and Greater Than 1

Another option for measuring variability of α using a geonium type experiment is to look for systems with Landé factors that are less than two and greater than one. The reason that this would be a useful system is that the spin flip frequency is now smaller than the cyclotron frequency. Because the spin flip frequency is now smaller it may be possible, within the constraints on the electric field of the trap, to make it equal to the cyclotron frequency. This can be seen by examining Eq. (7.106) again

$$\omega_c' = \frac{\omega_c}{2} + \frac{\omega_c}{2}\sqrt{1 - \frac{4amc^2}{B^2}}. \tag{7.110}$$

From this equation it can be shown that the range of the cyclotron frequency is $\omega_c/2 < \omega_c' < \omega_c$. The cyclotron frequency ω_c' of the trap varies as a, the strength of the electric field, and B, the strength of the magnetic field, vary. As a is increased the value of the cyclotron frequency decreases. Because the spin flip frequency is less than the cyclotron frequency for a system with $1 < g < 2$, increasing the electric field will bring the frequencies closer. If the frequencies are made equal the anomaly frequency of the trap is zero. This means that a measurement of the anomaly frequency will lead to infinite accuracy on the drift of the spin flip frequency assuming that the field strengths could be determined exactly. An infinite accuracy on the spin flip frequency would lead to an infinite accuracy on the variability of the fine structure constant.

The challenge is now to find a system with a Landé factor that is less than two and greater than one. Leptons can not be used. The Landé factor predicted by Dirac's equation for leptons is two. The only possibility of finding a lepton with a Landé factor less than two is for the anomalous magnetic moment to be negative. It should be noted that antiparticles have the opposite sign in their gyromagnetic ratio but the same sign in the anomaly. However, QED predicts that the first order contribution to the anomalous magnetic moment of all the leptons is the same. This is a positive value which leads to a positive anomalous magnetic moment for all leptons, whether particle or antiparticle.

The next simplest particles to consider are the nucleons. The two types of nucleons are the protons and the neutrons. The neutron has a Landé factor less than zero, namely -1.91. Since only the magnitude really matters this would work, however, because the neutron has no charge, there is no corresponding cyclotron frequency. Thus such measurements on the neutron are not possible. The proton on the other hand has a charge but its Landé factor has a value greater than two and therefore does not qualify either.

Our next consideration is to use atomic nuclei. The g factors of nucleons add approximately. This means that if a nucleus with $1 < g < 2$ and spin $1/2$ can be found it might be possible to create a system with a cyclotron frequency and a spin flip frequency that are equal. Searching for nuclear g factors we found only six different stable nuclei that satisfy the condition on g. They can be seen in table 7.1.

Although these atoms have the correct spin and their Landé factor fall within the acceptable range, there still may be some experimental problems associated with using them in the Penning trap experiment. In order to make these measurements, the atom must be completely ionized. The reason for this is that the electron magnetic moment is about 2000 times larger than the nuclear magnetic moment. If any electrons are present their magnetic moment would dominate. There is a large collection of literature using atomic geonium with atomic ions in a Penning trap[16, 17, 18, 19]. The second question that arises is to what extent a bare nucleus can be trapped in a Penning trap after all its electrons have been removed.

Z	Element	Atomic Number	Landé Factor	Lifetime	
15	Phosphorus	29	1.2349(3)	4.1 s	Not Stable
		31	1.13160(3)	Stable(100%)	Stable
50	Tin	117	1.00104(7)	Stable(7.7%)	Stable
		119	1.04728(7)	Stable(8.5%)	Stable
81	Thallium	203	1.62225787(12)	Stable(29.5%)	Stable
		205	1.63821461(12)	Stable(70.5%)	Stable

Table 7.1: Nuclei with $1 < g < 2$ and spin 1/2 (adapted from [31])

Assuming that such an experiment is possible a theoretical concern becomes to determine how the magnetic moment depends on the fine structure constant. The g factor of nuclei is dependent on contributions from quantum chromodynamics(QCD) as well as QED contributions. This means that a drift in the anomaly frequency could be detecting a varying strong coupling constant, as well as a varying fine structure constants, α. However, if the strong coupling constant is assumed to be time independent then a drift in the anomaly frequency can be assumed to be detecting the variation of alpha. On the other hand models of grand unification seem to imply that the time variation of the electromagnetic coupling constant α and the strong coupling constant should be correlated.

In order to determine the α dependence of the nucleus, consideration will be given to the nuclear moments of the proton and the neutron. The magnetic moment of a baryon is due to contributions from its three quarks labelled 1,2,3 as seen in the following relation[29]

$$\vec{\mu}_p = \vec{\mu}_1 + \vec{\mu}_2 + \vec{\mu}_3. \tag{7.111}$$

If quarks are Dirac particles (spin 1/2 particles with charge q and mass m) their magnetic moment will have a similar form to that of the electron

$$\vec{\mu_i} = \frac{q_i}{m_i}\vec{S}_i. \tag{7.112}$$

This leads to the magnitude of the magnetic moment of the quarks of

$$\mu = \frac{q\hbar}{2m}. \tag{7.113}$$

The magnetic moments for the up(u), down(d), and strange(s) quarks are given explicitly as

$$\begin{aligned} \mu_u &= \frac{2}{3}\frac{e\hbar}{2m_u c} = \frac{2}{3}\frac{m_e}{m_\mu}\mu_B, \\ \mu_d &= -\frac{1}{3}\frac{e\hbar}{2m_d c}, \\ \mu_s &= -\frac{1}{3}\frac{e\hbar}{2m_s c}. \end{aligned} \tag{7.114}$$

Knowing the quark magnetic moments, and using the wave function of the baryon $|B\uparrow\rangle$, the magnetic moment of the baryons can be calculated as follows

$$\mu_b = \langle B\uparrow|(\vec{\mu}_1 + \vec{\mu}_2 + \vec{\mu}_3)_z|B\uparrow\rangle = \frac{2}{\hbar}\sum_{i=1}^{3}\langle B\uparrow|\mu_i S_i|B\uparrow\rangle. \tag{7.115}$$

The wave function takes the following form for a proton

$$\frac{\sqrt{2}}{3}(u(\uparrow)u(\uparrow)d(\downarrow)) - \frac{1}{3\sqrt{2}}(u(\uparrow)u(\downarrow)d(\uparrow)) - \frac{1}{3\sqrt{2}}(u(\downarrow)u(\uparrow)d(\uparrow)) + \text{permutations}. \tag{7.116}$$

If the the sum in Eq. (7.115) is evaluated using the wave function in Eq. (7.116) and knowing that

$$\mu_1 S_z u(\uparrow) = \mu_1 \frac{\hbar}{2}u(\uparrow), \tag{7.117}$$

and

$$\mu_1 S_z u(\downarrow) = -\mu_1 \frac{\hbar}{2}u(\downarrow), \tag{7.118}$$

the following result is obtained

$$\mu_p = \frac{1}{3}(4\mu_u - \mu_d). \tag{7.119}$$

Using this method a value of 2.79 is obtained for the Landé factor of the proton. The actual value of the proton's magnetic moment is 2.793[29] which is in good agreement with theory. Using the same formalism for the neutron the magnetic moment is found to be

$$\mu_n = \frac{1}{3}(4\mu_d - \mu_u). \tag{7.120}$$

This predicts a Landé factor of -1.86 which is very close to the measured value of -1.913[29].

It may appear that the fine structure constant is not present in the nuclear magnetic moments. However, this calculation has ignored the radiative correction that would come from QED. The first order correction term for the analogous magnetic moment of Dirac particles comes from the analysis of the following Feynman diagram:

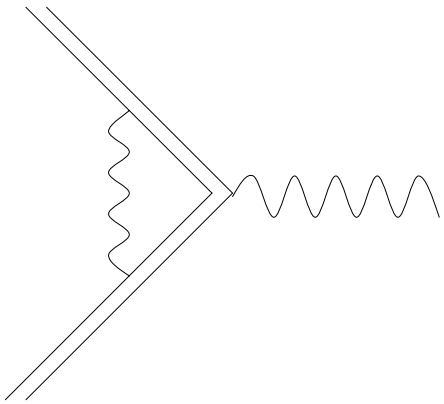

Figure 7.5: Feyman diagram for the quark-photon vertex

This leads to the Schwinger term for the contribution to the quark anomalous magnetic moment

$$\frac{q^2}{\hbar c 2\pi}. \tag{7.121}$$

The only difference in the Schwinger term, when using quarks as opposed to electrons, is that the charge would be $(2/3)e$ for the up quark and $(1/3)e$ for the down quark. Using the correction term from Eq. (7.121) to fix the values of the up quark and down quark magnetic moments we obtain

$$\mu_u \Rightarrow (1 + \frac{4\alpha}{9\pi})\mu_u, \tag{7.122}$$

and

$$\mu_d \Rightarrow (1 + \frac{\alpha}{9\pi})\mu_d. \tag{7.123}$$

Applying Eq.(7.122) and Eq. (7.123) to the expression for the magnetic moments, Eq. (7.119), leads to the following corrected magnetic moment $\widetilde{\mu_p}$

$$\widetilde{\mu_p} = \frac{1}{3}(4\mu_u - \mu_d) + \frac{1}{3}(\frac{16\alpha}{9\pi}\mu_u - \frac{\alpha}{9\pi}\mu_d). \tag{7.124}$$

Because the masses of the up and down quarks are approximately equal

$$\mu_u \approx -2\mu_d. \tag{7.125}$$

This means that Eq.(7.124) can be simplified to

$$\widetilde{\mu_p} \approx \mu_p - \frac{33\alpha}{27\pi}\mu_d, \tag{7.126}$$

where μ_p is the magnetic moment of the proton without the QED corrections. The corrected proton magnetic moment is 2.7924. This shows that the magnetic moment of the proton is dependent on the value of alpha. A similar calculation can be done for the neutron leading to a corrected magnetic moment for the neutron $\widetilde{\mu_n}$

$$\widetilde{\mu_n} \approx \mu_n + \frac{12\alpha}{27\pi}\mu_d, \tag{7.127}$$

where μ_n is the Landé factor of the neutron without the QED corrections. This leads to a predicted value for the neutron of 1.861.

Because the magnetic moment of the nucleons is dependent on the fine structure constant, the nuclear magnetic moment must also be dependent on the fine structure constant. This can be seen by examining the energy wells associated with the nucleons. The nucleons split into two separate energy wells for protons and neutrons. They are then paired up according to their spin. The nuclear magnetic moment is then approximately equal to that of the unpaired nucleons. We thus expect nuclear magnetic moments to be linearly dependent on the fine structure constant as a result of lowest order QED corrections as seen in Eq.(7.126) and Eq.(7.127).

Chapter 8

Comparison of the Three Methods

After having reviewed several methods for determining the variation of the fine structure constant, the question arises as to which method yields the highest precision. This will be determined by examining the three methods: the astrophysical method, the atomic clock method, and our newly proposed Penning trap method. Relevant data are summarized in table 8.1.

Field	Measurement	Order of Magnitude	Author
Astrophysics I	-5.8 ± 1.4	$10^{-16} yr^{-1}$	[8]
Astrophysics II	-0.65 ± 1.85	$10^{-16} yr^{-1}$	[11]
Atomic Clocks I	≤ 3.7	$10^{-14} yr^{-1}$	[22]
Atomic Clocks II	?	$10^{-18} yr^{-1}$	[23]
Oklo	0.4 ± 0.5	$10^{-17} yr^{-1}$	[18]

Table 8.1: The constraints on alpha variability (adapted from [8, 11, 22, 23, 18])

8.1 Astrophysical Advantages and Disadvantages

8.1.1 Advantages

Astrophysical experiments are very promising for measuring the variability of the fine structure constant. The sensitivity of the astrophysical measurements to a varying fine structure constant is due to the large comparison times that characterize

cosmology. Because it takes light several billion years to arrive at earth from distant galaxies, the light that is observed is very old. This allows physicists to look back in time and see what the universe was like in the past. The astrophysicist can obtain comparison times of up to 10^{10}yrs. Because the comparison times are so long, the actual change of alpha is many orders of magnitude larger than that obtained in earth bound experiments. This means that the required accuracy for a given sensitivity is much less. The other advantage of astrophysical observation is the nearly endless amount of data to be collected. Astrophysicists can collect huge data sets that will help them build their statistics, allowing them to reduce their error bars, and possibly find ways to throw out anomalies.

8.1.2 Disadvantages

Although it may seem that the advantages of astrophysical observation make it the obvious choice for detecting the variability of the fine structure constant, there are difficulties that greatly limit the accuracy obtained. The largest disadvantage of astrophysical measurements is the presence of large error bars. In fact the error bars for astrophysical data are so large that they almost completely offset the advantages associated with large time scales. Another disadvantage of astrophysical measurement is the large distance between the location of emission and that of detector. Because of this large distance the observer can never be certain whether the light was affected by other processes during its journey to the receiver on earth. Yet another disadvantage of astrophysical measurements is that the environment can not be controlled. This leaves a degree of uncertainty in what the astronomer is actually observing. This also means that the system can not be strained in order to optimize the outcome. In other words: the astronomers have to take what they get. Lastly, the astrophysical data are interpreted against very complex atomic calculations.

8.2 Atomic Clock Advantages and Disadvantages

8.2.1 Advantages

Using atomic clocks is currently the best method for measuring the variability of α in an earth bound experiment. The main advantage of atomic clocks is the level of accuracy in the data. The frequency of an atomic clock can be determined to 1 part in 10^{15}. This high precision allows experimentalists to currently probe the variability of alpha to $10^{-14} yrs^{-1}$.

Another advantage of atomic clocks is that the measurements are made on atoms. Atoms form microscopic traps for the electron with a very stable environment. The atom is ultimately a trap made by nature. These natural traps are all identical. This means that experimentalists do not have to worry about trap imperfections when working with atoms. The other advantage of the atomic clock experiment is the stability of the experiment. This high stability in time allows atomic clock physicists to make measurements for time frames up to a year. This leads to comparison times on the order of a year. Although this is short compared to cosmological time scales for an earth bound experiment this is quite long.

An advantage of any earth bound experiment, like the ones based on atomic clocks, is the added flexibility. The flexibility of atomic clocks comes from the freedom to choose from several atomic systems, when making an atomic clock measurement. Atomic physicists can optimize their results by determining the best atoms to compare. There is also flexibility found in the method of measurement. By using different methods to make measurements, increased sensitivity may be possible.

8.2.2 Disadvantages

The big disadvantage of atomic clocks, as compared to astrophysical observation, is the time scale. With a comparison time of $1yr$, the accuracy of the atomic clock measurements needs to be ten orders of magnitude better. This is obviously a large obstacle to overcome. Another challenge is the complexity of atomic bound states. The atomic theory of the fine structure splitting is very complicated and

therefore limited in accuracy. This means that experimentalists have to find a way to get around limitations in order to get precise predictions. An example of this can be seen in the ratio used by Prestage [22].

8.3 Advantages and Disadvantages of Penning Trap Methods

8.3.1 Advantages

The Penning trap is a very simple trap. This simplicity makes it optimal for designing precision measurements. One of the advantages of the geonium type experiments is the environment, the Penning trap, can be controlled. The experimentalist has nearly complete control of the electric and magnetic field configurations that confine the trapped particle. This allows experimentalists to get the most out of their experiments. This simplicity of the trap leads to a clean and neat theory. The wave function and energy of the electron can be found exactly in the Penning trap, at least in the non relativistic domain that we have considered. The Penning trap has the advantage of a stable environment as well. Physicists have been able to trap an electron in the Penning trap for several months. This time frame is of the order of that of the atomic clock experiments.

The Penning trap has a significant amount of flexibility. The flexibility of the Penning trap comes from two features of the experiment. Just like the atomic physicists are able to chose what type of atom to use in their clock, an experimentalist using a Penning trap can choose what type of particle to use, including composite systems like an atom or the nucleus of an atom. Another flexibility of the Penning trap is that it allows for control of the fields. This means that experimentalists can create an environment that will magnify the features they are searching for. This is probably the most significant advantage.

8.3.2 Disadvantages

The disadvantages of the Penning trap are threefold. The largest disadvantage is in the comparison times. The comparison times are of the same order as that of the atomic clocks. This means that measurements made in the Penning trap must be at

least 10 orders of magnitude more accurate in order to compete with the astrophysical measurements.

The second disadvantage comes from trap stability. Because the Penning trap is man made, it has associated imperfections. These errors are due to the uncertainty in the field configuration. This uncertainty is present because the electrodes in the experiment can never be perfectly machined nor perfectly aligned. This uncertainty in the field configuration puts a constraint on the accuracy of the frequency measurements. However, the Penning trap has a feature that is able to minimize this disadvantage. In the Penning trap, if the following condition is present,

$$\omega_m \neq \frac{\omega_z^2}{2\omega_c'}, \tag{8.1}$$

then the experimentalist knows that the trap is not properly machined and/or aligned. This allows for correcting the problem.

A third disadvantage is that the theory for the magnetic moment being measured is complicated. For leptons this is not a problem as QED is well understood. However, for composite particles such as baryons, nuclei and atoms the theory is messy and not completely understood, as they involve QCD and multielectron bound state QED. Of course, bringing in new parameters, like α_{QCD}, can lead to false interpretations of α variability, as the new parameters could themselves be time dependent. This leads to an added uncertainty in the measurements being made.

8.4 An Ultimate Experiment?

Our discussion leads to the question as to what might be the ultimate experiment. The ultimate experiment would have large comparison times, just as in astrophysics. The trap would also need to be without flaws, just as an atom is. The perfect experiment would also give the experimentalist control of the field configuration, just as the Penning trap does. This means that the best method for determining the variability of α would be a naturally occurring geonium trap without flaws that is present in quasars. Until we have found such a system we will have to continue to improve the three methods discussed in this chapter separately.

Chapter 9

Conclusion

This thesis has shown that, if the fine structure constant is time dependent, current theories may have to be be drastically remolded or even abandoned. It has revealed the fact that $g-2$ experiments from the past fifty years lack the accuracy necessary to put a constraint on the variability of alpha. It has also shown that a Penning trap containing leptons has many difficulties to overcome if a competitive measurement of α variability is to be made. However, if composite particles are considered, it may be possible to create a competitive experiment for measuring the variability of α. Another aspect of the trap that is promising is to look at the relativistic solution in the trap. Because of the link between spin-flip and cyclotron frequency in this regime, new methods to measure α variability may become possible. This should be the subject of future work. It may be possible to use our proposal on nuclei, and adapt it to the bound electron Landé factor experiments[16, 17, 18]. This should also be a subject of future work.

Appendix A

The Free Electron Landé Factor

One of the great triumphs of relativistic quantum theory, namely the Dirac equation, was that it predicted that the Landé factor was 2. This feature of the Dirac equation, however, is not obvious. In order to extract the Landé factor, we start with Dirac's equation with minimal coupling[1]

$$[\not{p} - e\ \not{A} - m]\Psi = 0, \tag{A.1}$$

then multiply this equation by $[\not{p} - e\ \not{A} + m]$ to get

$$[(\not{p} - e\ \not{A})^2 - m^2]\Psi = 0. \tag{A.2}$$

The equation is then expanded to give

$$[\not{p}^2 + e^2\ \not{A}^2 - e\,(\not{p}\ \not{A} + \not{A}\ \not{p}) - m^2]\Psi = 0. \tag{A.3}$$

Simplification occurs when we separate the symmetric and antisymmetric parts of the product of gamma matrices

$$\gamma^\mu\gamma^\nu = g^{\mu\nu} + i\sigma^{\mu\nu}, \tag{A.4}$$

and substitute this expression into Eq.(A.3) to get

$$[p^2 + e^2A^2 - e\,(g^{\mu\nu} + i\sigma^{\mu\nu})\,(p_\mu A_\nu + A_\mu p_\nu) - m^2]\Psi = 0. \tag{A.5}$$

[1]In the appendices, $c = 1$, $\hbar = 1$ $\not{p} \equiv \gamma^\mu p_\mu$, and γ^μ are the Dirac matrices (see ref [15] for more details), Greek indices vary from 0 to 3 and Latin indices vary from 1 to 3.

If the previous expression is expanded, the term containing $\sigma^{\mu\nu}$ can be shown to be

$$i\sigma^{\mu\nu}\left(p_\mu A_\nu + A_\mu p_\nu\right) = -\sigma^{\mu\nu}F_{\mu\nu}. \tag{A.6}$$

This leads to the following form of the second order Dirac equation

$$\left[p^2 + e^2A^2 - e\left(p^\mu A_\mu + A^\mu p_\mu\right) + e\sigma^{\mu\nu}F_{\mu\nu} - m^2\right]\Psi = 0. \tag{A.7}$$

Eq. (A.7) can be simplified using the following relations[20]

$$\sigma^{0k} = i\alpha^k, \tag{A.8}$$

$$\sigma^{ij} = i\epsilon^{ijk}\sigma^k, \tag{A.9}$$

and

$$\sigma^{\mu\mu} = 0, \tag{A.10}$$

where σ^k is a 2×2 matrix with the k^{th} Pauli matrix on the diagonal, and $\alpha^k = \gamma^0\gamma^k$:

$$\left[p^2 + e^2A^2 - e\left(p^\mu A_\mu + A^\mu p_\mu\right) - ie\vec{\alpha}\cdot\vec{E} + e\vec{\sigma}\cdot\vec{B} - m^2\right]\Psi = 0. \tag{A.11}$$

In the previous equation the electric field $\vec{E}$ and the magnetic field $\vec{B}$ are defined as (compare Eq.(7.76))

$$\begin{aligned} B_k &= \epsilon_{ilm}F^{lm} = i\epsilon_{ijk}(p_iA_j + A_ip_j) \\ E_k &= F_{0k} = \frac{p_0A_i + p_iA_0}{i} \end{aligned} \tag{A.12}$$

where

$$A_0 = \phi. \tag{A.13}$$

It is now clear that the term with the $\sigma^{\mu\nu}$ in Eq.(A.7) is the origin of the $\vec{\sigma}\cdot\vec{B}$ term in Eq.(A.11). It will be shown that this term leads to the magnetic moment of the particle.

The previous expression (A.11) can be put in the form of the Klein-Gordon equation with minimal coupling plus spin in the following way

$$\left[(\varepsilon - e\Phi)^2 - (\vec{p} - e\vec{A})^2 - ie\vec{\alpha}\cdot\vec{E} + e\vec{\sigma}\cdot\vec{B} - m^2\right]\Psi = 0, \tag{A.14}$$

where ε is the energy coming from the time derivative operator, $\vec{E}$ is the electric field, $\vec{p}$ is the three momentum, and $\vec{B}$ is the magnetic field. The non relativistic limit will be taken in order to show that the $\vec{\sigma}\cdot\vec{B}$ is the source of the magnetic moment. This is done by decomposing the wave function into upper and lower comonents[20]

$$\psi = \begin{pmatrix} \chi \\ \xi \end{pmatrix}. \tag{A.15}$$

The Dirac equation decouples leads to two coupled equations

$$\begin{aligned} (\varepsilon - e\Phi - m)\chi - \vec{\sigma}\cdot(\vec{p} - e\vec{A})\xi = 0 \\ (\varepsilon - e\Phi + m)\xi - \vec{\sigma}\cdot(\vec{p} - e\vec{A})\chi = 0 \end{aligned} \tag{A.16}$$

The lower component, ξ, of the wave function corresponds to the contribution associated with antiparticles and is very small in the non relativistic limit. ξ can be extracted from the second equation in A.17

$$\xi = \frac{\vec{\sigma}\cdot(\vec{p} - e\vec{A})\chi}{(E - e\phi + m)} \tag{A.17}$$

A similar decomposition of the 2^{nd} order Dirac equation, Eq.(A.14) gives

$$\begin{aligned} \left[(\varepsilon - e\Phi)^2 - (p - eA)^2 + e\vec{\sigma}\cdot\vec{B} - m^2\right]\chi + ie\vec{\sigma}\cdot\vec{E}\xi = 0 \\ \left[(\varepsilon - e\Phi)^2 - (p - eA)^2 + e\vec{\sigma}\cdot\vec{B} - m^2\right]\xi - ie\vec{\sigma}\cdot\vec{E}\chi = 0 \end{aligned} \tag{A.18}$$

where $\vec{\sigma}$ are now regular Pauli matrices. If Eq.(A.17) is substituted into the first relation in Eq.(A.19), we obtain a decoupled exact equation for the upper components

$$\left[(\varepsilon - e\Phi)^2 - (p - eA)^2 + e\vec{\sigma}\cdot\vec{B} - m^2\right]\chi - ie\vec{\sigma}\cdot\vec{E}\frac{\vec{\sigma}\cdot(\vec{p} - e\vec{A})\chi}{(E - e\Phi + m)} = 0. \tag{A.19}$$

When taking the non relativistic limit, the following substitution is made to acknowledge the fact that the definition of the non relativistic energy ϵ does not include the rest energy m

$$E = m + \epsilon, \tag{A.20}$$

in Eq. (A.19) with the assumption that $\epsilon \ll m$ and $e\Phi \ll m$ (weak field). After making the non relativistic ($\epsilon \ll m$) and weak field ($e\Phi \ll m$) assumption and keeping only terms up to first order in ϵ and Φ, Eq.(A.19) becomes

$$\begin{aligned}&\left[m^2 - 2e\Phi m + 2\epsilon m - (p - eA)^2 + e\vec{\sigma}\cdot\vec{B} - m^2\right]\chi \\ &+\left[\frac{e}{2m}\vec{\sigma}\cdot\vec{E_f}\times(\vec{p} - e\vec{A}) - \frac{ie}{2m}\vec{E_f}\cdot(\vec{p} - e\vec{A})\right]\chi = 0.\end{aligned} \tag{A.21}$$

The terms that are divide by m can be ignored in this non relativistic approximation because they are small compared to the other terms. This leads to a Pauli like equation

$$\left[e\Phi - \epsilon + \frac{1}{2m}(p - eA)^2 - \frac{e}{2m}\vec{\sigma}\cdot\vec{B}\right]\chi = 0. \tag{A.22}$$

Examining the term with the sigma matrices, it can be seen that the Landé factor is 2 just as expected. It should be emphasized that this exact result was obtained from the *nonrelatvistic* limit of the Dirac equation. In contrast the contribution of the anomalous magnetic moment necessitates a fully relativistic calculation as explained in Appendix B.

Appendix B

Anomalous Magnetic Moment of the Free Electron

This section is inspired by the treatment found in Ryder [15] and Huang [20]. The anomalous magnetic moment is found by considering corrections to the defining vertex of QED. The Feynman diagram for this vertex of QED can be seen in figure 4.1.

Feynman rules tell us that the elementary vertex corresponds to a factor of $ie\gamma_u$. This factor can be decomposed into a momentum and a magnetic moment term through Gordon decomposition of the current

$$\overline{u(p')}\left[\gamma_\sigma\right]u(p) = \overline{u(p')}\left[\frac{p_\sigma + p'_\sigma}{2m} + \frac{iq_\nu\sigma_{\mu\nu}}{2m}\right]u(p). \tag{B.1}$$

As shown in Appendix A, the magnetic moment is present in the term that contains the $\sigma_{\mu\nu}$ matrix. This means that the bare vertex in QED contains the magnetic moment with a Landé factor of two just as Dirac predicted. In order to find the anomalous magnetic moment, the corrections to the vertex need to be calculated. This implies a transformation

$$\gamma_\sigma \Rightarrow \gamma_\sigma + \Lambda_\sigma \tag{B.2}$$

The diagram for the first order correction to the vertex can be seen in figure 4.2.

Feynman rules tell us that the photon propagator contributes a factor $-ig^{\mu\nu}/k^2$, where k is the 4-momentum of the photon, which corresponds to the sinusoidal line in the diagram and that the Dirac propagator contributes a factor $i/(\not{p} - m)$ which

corresponds to the straight line. Using these rules, the Feynman diagram without the legs can be converted into an integral expression,

$$I = (-ie)^3 \int \frac{d^4k}{(2\pi)^4} \frac{-ig^{\mu\nu}}{k^2} \gamma_\mu \frac{i}{(\not{p} - \not{k}) - m} \gamma_\sigma \frac{i}{(\not{p}' - \not{k}) - m} \gamma_\nu. \tag{B.3}$$

The gamma matrices are removed from the denominator using the following relation

$$\frac{1}{(\not{p} - \not{k}) - m} = \frac{(\not{p} - \not{k}) + m}{(\not{p} - \not{k})^2 - m^2} \tag{B.4}$$

which leads after some simplification to

$$I = -(e)^3 \int \frac{d^4k}{(2\pi)^4} \frac{g^{\mu\nu}\gamma_\mu((\not{p} - \not{k}) + m)\gamma_\sigma((\not{p}' - \not{k}) + m)\gamma_\nu}{k^2((p-k)^2 - m^2)((p'-k)^2 - m^2)}. \tag{B.5}$$

In order to perform this integral the expression is converted to a triple integral

$$I = \frac{-2(e)^3}{(2\pi)^4} \int_0^1 dx \int_0^{1-x} dy \int d^4k \frac{g^{\mu\nu}\gamma_\mu((\not{p} - \not{k}) + m)\gamma_\sigma((\not{p}' - \not{k}) + m)\gamma_\nu}{(k^2(1-x-y) + ((p-k)^2 - m^2)x + ((p'-k)^2 - m^2)y)^3} \tag{B.6}$$

where the identity Eq.(B.7) has been used.

$$\frac{1}{abc} = 2 \int_0^1 dx \int_0^{1-x} dy \frac{1}{(a(1-x-y) + bx + cy)^3} \tag{B.7}$$

Simplification of the denominator followed by the substitution $k = k' - px - p'y$ leads to the integral expression

$$I = \frac{-2(e)^3}{(2\pi)^4} \int_0^1 dx \int_0^{1-x} dy \int d^4k' \frac{\gamma^\nu(\not{p}(1-x) - \not{p}'y - \not{k}' + m)\gamma_\sigma(\not{p}'(1-y) - \not{p}x - \not{k}' + m)\gamma_\nu}{(k'^2 - (px + p'y)^2 + p^2x + p'^2y - m^2(x+y))^3}. \tag{B.8}$$

When the numerator is expanded it has terms that are quadratic, linear, and independent of k'. The terms linear in k' integrate out. The terms quadratic in k' are divergent and are cancelled by counterterms in the Lagrangian in the renormalization

procedure. The term independent of k' is the only piece that contribute to the anomalous magnetic moment. The integral corresponding to this term, I_0, takes the following form

$$I_0 = \frac{-2(e)^3}{(2\pi)^4} \int_0^1 dx \int_0^{1-x} dy \int d^4k' \frac{\gamma^\nu(\not{p}(1-x) - \not{p}'y + m)\gamma_\sigma(\not{p}'(1-y) - \not{p}x + m)\gamma_\nu}{(k'^2 - (px+p'y)^2 + p^2x + p'^2y - m^2(x+y))^3} \tag{B.9}$$

The integral over k' can be evaluated using the following d-dimensional integral expression

$$\int \frac{d^dp}{(p^2 - 2pq - m^2)^\alpha} = (-1)^{\frac{d}{2}} i\pi^{\frac{d}{2}} \frac{\Gamma(\alpha - \frac{d}{2})}{\Gamma(\alpha)} \frac{1}{(-q^2 - m^2)^{\alpha - \frac{d}{2}}} \tag{B.10}$$

with $\alpha = 3$ and $d = 4$, and yields

$$I_0 = \frac{-i(e)^3}{16\pi^2} \int_0^1 dx \int_0^{1-x} dy \frac{\gamma^\nu(\not{p}(1-x) - \not{p}'y + m)\gamma_\sigma(\not{p}'(1-y) - \not{p}x + m)\gamma_\nu}{(px+p'y)^2 - p^2x + p'^2y + m^2(x+y))^3}. \tag{B.11}$$

This expression now leads to an expression involving products of three, four and five gamma matrices. The integral in Eq. (B.11) can be simplified using the gamma matrix contraction identities in table B.1, after which at most three gamma matrices will remain. Further simplification is obtained through multiplication on the left by $\overline{u}(p')$ and on the right by $u(p)$. Then using the anti-commutation relations of the γ_μ matrices, we move all $\not{p}'$ factors in the numerator to the left so that they may act on $\overline{u}(p')$ and move all $\not{p}$ factors to the right so that they may act on $u(p)$. Since the end legs of the Feynman diagram correspond to free particles, satisfying the free Dirac equations

$$\not{p}u(p) = mu(p), \tag{B.12}$$

and

$\gamma_\lambda \gamma^\alpha \gamma^\lambda = -2\gamma^\alpha$
$\gamma_\lambda \gamma^\alpha \gamma^\beta \gamma^\lambda = 4g^{\alpha\beta}$
$\gamma_\lambda \gamma^\alpha \gamma^\beta \gamma^\delta \gamma^\lambda = -2\gamma^\alpha \gamma^\beta \gamma^\delta$

Table B.1: Useful identities

$$\overline{u}(p') \not{p}' = m\overline{u} \tag{B.13}$$

the convergent part of the numerator of Eq. (B.11) becomes

$$-4mp'_\sigma[y^2 - y + xy] - 4mp_\sigma[x^2 - x + xy] - 4m(x-y)[p_\sigma - p'_\sigma]. \tag{B.14}$$

The denominator can be simplified by using the on mass-shell condition for the external legs

$$\sqrt{p^2} = \sqrt{p'^2} = m. \tag{B.15}$$

This allows the denominator to simplify to $m^2(x+y)^2$. Combining the simplified expressions of the denominator with the terms in Eq. (B.14) implies that the vertex modification from Eq.(B.2) becomes

$$ie\Lambda^{(2)}_\sigma = \frac{ie^3}{4\pi^2 m}\int_0^1 \int_0^{1-x} \frac{(-p'_\sigma[y^2 - y + xy] - p_\sigma[x^2 - x + xy] - (x-y)[p_\sigma - p'_\sigma])}{(x+y)^2}. \tag{B.16}$$

When the integrals are performed the value for the correction to the vertex is

$$\Lambda^{(2)}_\sigma = \frac{-e^2}{16\pi^2 m}(p_\sigma + p'_\sigma) = \frac{\alpha}{4\pi m}(p_\sigma + p'_\sigma), \tag{B.17}$$

where

$$\alpha = \frac{e^2}{4\pi}. \tag{B.18}$$

Using the Gordon decomposition for the current on the corrected vertex term gives

$$u(p')\left[-\frac{\alpha}{4\pi m}(p_\sigma + p'_\sigma)\right]u(p) = u(p')\left[\gamma_\sigma\frac{-\alpha}{2\pi} + \frac{\alpha}{2\pi}\frac{iq_\nu\sigma_{\mu\nu}}{2m}\right]u(p). \tag{B.19}$$

As was seen in Appendix A, the factors multiplying the $\sigma^{\mu\nu}$ give the magnetic moment in the nonrelativistic limit thus leading to a total expression for the Landé factor of

$$\frac{g}{2} = (1 + \frac{\alpha}{2\pi}). \tag{B.20}$$

Bibliography

[1] Uzan, J.P., 2003, Rev. Mod. Phys. 75, 403.

[2] Mohr, P.J. and B.N. Taylor, 1999, J. Phys. Chem. Ref. Data 28, 1713.

[3] Dirac P.A.M., 1937, Nature (London) 139, 323.

[4] Dyson, F.J., 1967, Phys. Rev. Lett. 19, 1291.

[5] Teller, E., 1948, Phys. Rev. 73, 801.

[6] Marciano, W., 1984, Phys. Rev. Lett., 52, 489.

[7] Webb *et al.*, 2003, Astrophys. Space Sci. 283, 565.

[8] Webb *et al.*, 2001, Phys. Rev. Lett. 87, 091301.

[9] Webb *et al.*, 1999, Phys. Rev. Lett. 82, 884.

[10] Sokolov, A. A. and Y.G. Pavlenko, 1967, Opt. Spectrosc. (USSR) 22, 1.

[11] Srianand *et al.*, 2004, Phys. Rev. Lett. 92, 121302.

[12] E. Merzbacher, *Quantum Mechanics*, (John Wiley & Sons, Inc., New York, 1998).

[13] Sommerfeld, 1916, A. Ann. Phys. (Leipzig) 51, 17, 1.

[14] D. Griffiths, *Introduction to Quantum Mechanics*, (Prentice Hall, New Jersey, 2000).

[15] L. Ryder, *Quantum Field Theory*, (Cambridge, Cambridge, 1996).

[16] Verdú et al., 2004, Phys. Rev. Lett. 92, 093002.

[17] Shabaev, V. M. and V. A. Yerokhin, 2002, Phys. Rev. Lett. 88, 091801 (2002).

[18] Fujii et al., 2002, http://arxiv.org/abs/hep-ph/0205206.

[19] Häffner *et al.*, 2000, Phys. Rev. Lett. 85, 5308.

[20] K. Huang, *Quantum Field Theory: From Operators to Path Integrals*, (John Wiley & Sons, Inc., New York, 1998).

[21] Murphy, *et al.*, 2001, Mon. Not. R. Astron. Soc. 327, 1208.

[22] Prestage *et al.*, 1996, Phys. Rev. Lett. 74, 3511.

[23] Nguyen *et al.*, 2004, Phys. Rev. A 69, 022105.

[24] Sortais, *et al.*, 2001, Physica Scripta T95, 50.

[25] Durfee, D. and S. Bergeson private communication.

[26] http://athena-positrons.web.cern.ch/ATHENA-positrons/wwwathena/penning.html.

[27] Lautrup, B and H. Zinkernagel, 1999, Stud. Hist. Phil. Mod. Phys., Vol 30, 85.

[28] Kinoshita, T, 1996, Rep. Prog. Phys. 59, 1459.

[29] D. Griffiths, *Introduction to Elementary Particles*, (John Wiley & Sons, Inc., New York, 1987).

[30] Du Toit, P., 2002, Honors Thesis Brigham Young University.

[31] http://atom.kaeri.re.kr/ton/main.shtml.

[32] Van Dyck *et al.*, and H.G. Dehmelt, 1986, Atomic Phys. 9, 53.

[33] Dehmelt, H. (1989a) "Geonium Spectra, Electron Radius, Cosmon" in *High Energy Spin Physics*, 8th International Symposium, K. Heller, Ed. (AIP Conference Proceedings No. 187, New York) p. 319.

[34] Peres, A, 2002, arXiv:gr-qc/0210066 v2 23 Oct 2002.

[35] http://www.phys.vt.edu/ jhs/faq/quasars.html May 2004.